BILINGUAL PUBLISHING CO.
Pioneer of Global Academics Since 1984

Journal of Botanical Research

Volume 4 | Issue 3 | July 2022 | ISSN 2630-5054（Online）

BILINGUAL PUBLISHING CO.
Pioneer of Global Academics Since 1984

Volume 4 Issue 3 • July 2022 • ISSN 2630-5054 (Online)

Journal of Botanical Research

BILINGUAL PUBLISHING CO.
Pioneer of Global Academics Since 1984

BILINGUAL PUBLISHING CO.
Pioneer of Global Academics Since 1984

Volume 4 | Issue 3 | July 2022 | Page1-43
Journal of Botanical Research

Contents

Articles

BILINGUAL PUBLISHING CO.
Pioneer of Global Academics Since 1984

Journal of Botanical Research
https://ojs.bilpublishing.com/index.php/jbr

ARTICLE

Correlation and Path Coefficient Analyses of Yield in Cacao (*Theobroma cacao* L.)

Omotayo Olalekan Adenuga* **Abigail Funlayo Adepoju** **Ibrahim Olalekan Sobowale** **Olayinka Olufemi Olaniyi** **Oluwatobi James Areola** **Terkula Felix Nyamkyume**

Plant Breeding Department, Cocoa Research Institute of Nigeria, Ibadan, 23401, Nigeria

ARTICLE INFO

Article history
Received: 5 May 2022
Revised: 9 June 2022
Accepted: 13 June 2022
Published Online: 12 July 2022

Keywords:
Cacao
Yield
Correlation
Phenotypic traits
Path coefficients

ABSTRACT

Cacao (*Theobroma cacao* L.) is an important commodity tree crop which produces the cocoa bean, a major source of income for most West African countries and many smallholder farmers. Declining yield of cacao is a major limitation to cocoa production in Nigeria. This study aimed at determining the correlations of the phenotypic traits that were related in the yield of the cacao genotypes. Nine cacao hybrids produced from some high-yielding parents in the research farm of Cocoa Research Institute of Nigeria, Ibadan, Nigeria were evaluated from 2012 through 2017 in Owena (7°11' N, 5°1' E), Ondo state, Nigeria. Character Correlations and Path Coefficient Analysis were used in the description of the performance of the genotypes. The study concluded that significant genotypic and phenotypic correlations existed among many of the pairs of the fruit and bean characters with one another and with pod index, suggesting a complex contribution of these characters either positively or negatively to growth and yield in cacao, and that fruit and bean traits are determinants of yield in cacao.

1. Introduction

The importance of the cacao crop is very enormous to farmers and government in the producing countries. Cocoa bean, the main ingredient used in the manufacture of chocolate, other beverages and confectionery products, is the major product obtained from the cacao tree. Declining yield is, however, a limiting factor in cacao cropping in Nigeria [1]. The cocoa bean yield is the primary focus of any cacao farming venture, and is indicated essentially in the "pod index", which refers to the number of cocoa pods (fruit) required to produce one kilogramme (1kg) of dry cocoa beans. Among other factors, cocoa bean yield is influenced by variety and age of plant [2]. A number of

*Corresponding Author:
Omotayo Olalekan Adenuga,
Plant Breeding Department, Cocoa Research Institute of Nigeria, Ibadan, 23401, Nigeria;
Email: tayoadenuga526@yahoo.com

DOI: https://doi.org/10.30564/jbr.v4i3.4694

factors are, therefore, observed to be correlated with pod index in cacao. Understanding the magnitude and direction of the association of the traits that influence yield, as a complex trait, is paramount in selection for improved yield [3].

Correlation is a measure of the degree of relationship between variables and a plant breeder should know whether the improvement of one character will result in simultaneous change in other characters through estimates of inter character correlations [4]. Estimates of genotypic, phenotypic and environmental correlations among characters can provide the basis of planning of more efficient breeding programmes. A positive genetic correlation between two desirable traits simplifies the breeder's job of crop improvement. As yield, being a complex and polygenic trait, is influenced even by fluctuations in environmental factors, a knowledge of the nature and magnitude of the traits that influence yield in cacao can provide a basis for genotype selection. Beyond the influence of climate, an often complex inter-relationship of plant traits is an important determinant of yield in cacao [1]. Therefore this study was carried out to understand the association among yield and the related traits in cacao so as to enhance further selection for the improved yield of the crop.

2. Materials and Methods

Nine new early-bearing cacao hybrids produced at the Cocoa Research Institute of Nigeria which fruited at the Owena sub-station (7° 11'N, 5° 1'E) of the Institute, with harvest period ranging from 104 through 124 weeks after field ploanting (Table 1) were used this study. Thirty (30) individual seedlings were established per genotype as ten (10) seedlings per plot in three (3) replications in a Randomized Complete Block Design (RCBD). Prior to fruit harvest, data were collected (at three months interval) on plant height, stem diameter, number of leaves, time to jorquette, jorquette height, tree circumference, fruiting and cherelle wilt. Five uniformly matured and ripe cocoa pods were harvested per genotype in each of three replications, giving a total of fifteen pods (fruits) per genotype. The time to fruit harvest (being the time of fruit maturation) was recorded in weeks. Each fruit was weighed, and the fruit length and width measured using a vernier calliper. The fruits were carefully broken and pod husk thickness was estimated as the difference between the outer (ridge to ridge) and the inner diameter of the fresh pod husk using the venier calliper. The number of rows, number of beans per row and number of beans per pod was counted and the weight of the beans was recorded per fruit, while the weight of one bean was recorded as the average of the weight of ten beans randomly selected per fruit. The beans from each fruit were extracted and fermented in trays. The beans were weighed after fermentation and the weight recorded per fruit and per individual bean as the average of ten fermented beans weighed. The fermented beans were sun-dried, and the pod value recorded as the weight of the total dried beans obtained per fruit. The weight of one dried bean was also recorded as the average of the weight of ten dried bean per fruit. Dried bean length and width were recorded by as an average of the values of ten dried beans using the vernier calliper.

Table 1. List of nine cacao genotypes used in the study

S/N	Genotypes	Pedigree	Weeks to Harvest
1	$P_1 \times P_{10}$	$(T_{82/27} \times T_{12/11}) \times (T_{65/7} \times T_{57/22})$	122
2	$P_1 \times P_{11}$	$(T_{82/27} \times T_{12/11}) \times (T_{53/5} \times {}_{N38})$	117
3	$P_2 \times P_{10}$	$(P_7 \times T_{60/887}) \times (T_{65/7} \times T_{57/22})$	124
4	$P_3 \times P_{10}$	$(T_{86/2} \times T_{9/15}) \times (T_{65/7} \times T_{57/22})$	114
5	$P_3 \times P_{11}$	$(T_{86/2} \times T_{9/15}) \times (T_{53/5} \times {}_{N38})$	105
6	$P_5 \times P_9$	$(T_{86/2} \times T_{22/28}) \times (T_{65/7} \times T_{22/28})$	117
7	$P_6 \times P_{10}$	$(T_{65/7} \times T_{9/15}) \times (T_{65/7} \times T_{57/22})$	104
8	$P_7 \times P_8$	$(P_7 \times P_{A150}) \times (T_{101/15} \times N_{38})$	117
9	$P_7 \times P_{10}$	$(P_7 \times P_{A150}) \times (T_{65/7} \times T_{57/22})$	114

Pod index was calculated from the weight of dried beans from each pod as the number of pods required to produce one kilogramme of dry cocoa beans. In all, a total of fourteen quantitative traits were used to assess the nine genotypes. The characters measured in cocoa pod and bean metrics and their units are presented in Table 2. The means from the sampling unit per genotype were used to estimate the phenotypic, genotypic and environmental correlation coefficients using the formula: of Miller *et al*. [5] thus:

$$r(x, y) = \frac{Cov(xy)}{\sqrt{(\delta x)^2.(\delta y)^2}}$$

where $r_{(x,y)}$ is either genotypic or phenotypic or environmental correlation between variables x and y;
$Cov_{(xy)}$ is the covariance of variables x and y;
$(\delta_x)^2$ is either the genotypic or phenotypic or environmental variance of variable x;
$(\delta_y)^2$ is either the genotypic or phenotypic or environmental variance of variable y.

The significance of the correlation coefficients was tested using the non-directional probability in the software of Lowry [6].

The traits which had significant genotypic correlation coefficients with Pod Index (the yield parameter) were subjected to Path Coefficient analysis by dissecting the correlations so as to understand the direct path of relationships between each trait and Pod Index, as well as the indirect path of relationship of each trait through other traits with Pod Index. The direct and indirect Path Coefficients were calculated to reveal the strength of the relationship among Pod Index and the yield-related traits by solving a series of simultaneous equations as suggested by Dewey and Lu [7].

Figure 1 shows the cause and effect system between independent and dependent variables. It reveals that pod index (X_{13}) was determined by Plant height (X_1), Stem diameter (X_2), Time to joruette (X_3), Jorquette height (X_4), Tree circumference (X_5), Presence of fruit (X_6), Cherelle wilt (X_7), Time to fruit harvest (X_8), Fruit weight (X_9), Fruit length (X_{10}), Fruit width (X_{11}), Number of Beans per row (X_{12}) and a composite variable (residual effect = U) that include all other factors affecting dry bean yield but not accounted for in this study.

Table 2. Characters measured in cocoa pod and bean metrics and their units

S/N	Character	Unit
1.	Time to fruit harvest	Weeks
2.	Fruit weight	Grammes
3.	Fruit Length	Millimetres
4.	Fruit Width	Millimetres
5.	Pod Thickness	Millimetres
6.	Number of rows	Nil
7.	Number of beans per row	Nil
8.	Number of beans per fruit	Nil
9.	Weight of beans per fruit	Grammes
10.	Weight of 1 bean	Grammes
11.	Weight of beans per fruit after fermentation	Grammes
12.	Weight of 1 bean after fermentation	Grammes
13.	Pod value (Total weight of dry beans per pod)	Grammes
14.	Weight of 1 dry bean	Grammes
15.	Dry bean length	Millimetres
16.	Dry bean width	Millimetres
17.	Pod index	Nil

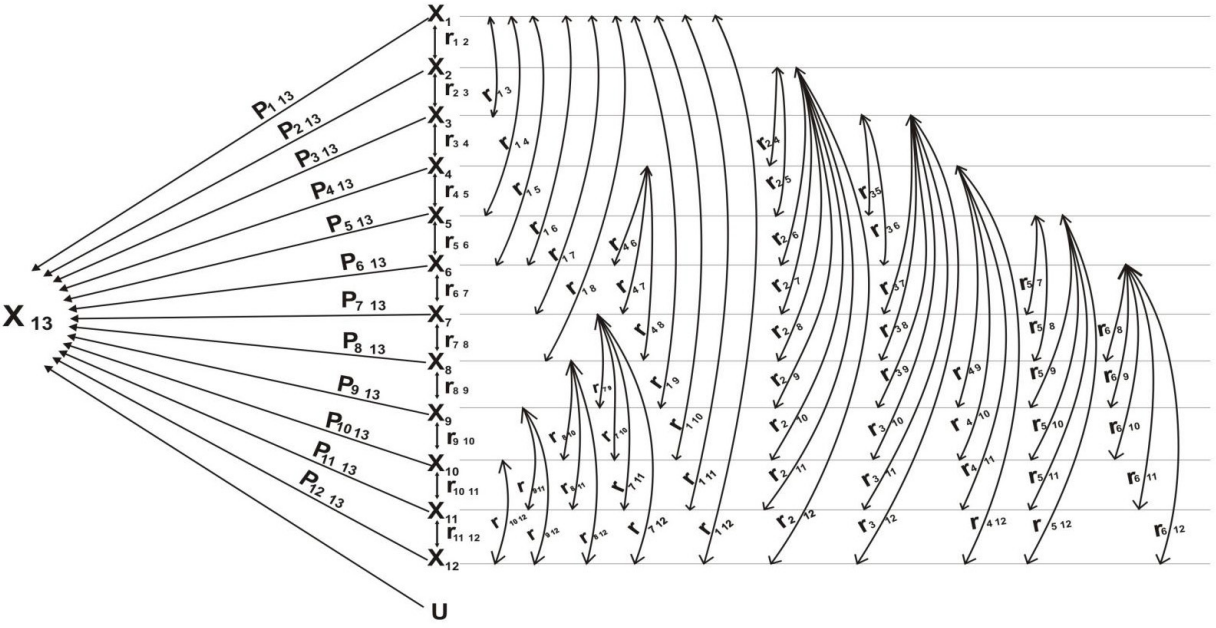

Figure 1. Causation diagram indicating the relationship between pod index and yield-related traits

From this figure,

$$r_{1\,13} = P_{1\,13} + r_{1\,2}P_{2\,13} + r_{1\,3}P_{3\,13} + r_{1\,4}P_{4\,13} + r_{1\,5}P_{5\,13} + r_{1\,6}P_{6\,13} + r_{1\,7}P_{7\,13} + r_{1\,8}P_{8\,13} + r_{1\,9}P_{9\,13} + r_{1\,10}P_{10\,13} + r_{1\,11}P_{11\,13} + r_{1\,12}P_{12\,13}$$

$$r_{2\,13} = r_{1\,2}P_{1\,13} + P_{2\,13} + r_{2\,3}P_{3\,13} + r_{2\,4}P_{4\,13} + r_{2\,5}P_{5\,13} + r_{2\,6}P_{6\,13} + r_{2\,7}P_{7\,13} + r_{2\,8}P_{8\,13} + r_{2\,9}P_{9\,13} + r_{2\,10}P_{10\,13} + r_{2\,11}P_{11\,13} + r_{2\,12}P_{12\,13}$$

$$r_{3\,13} = r_{1\,3}P_{1\,13} + r_{2\,3}P_{2\,13} + P_{3\,13} + r_{3\,4}P_{4\,13} + r_{3\,5}P_{5\,13} + r_{3\,6}P_{6\,13} + r_{3\,7}P_{7\,13} + r_{3\,8}P_{8\,13} + r_{3\,9}P_{9\,13} + r_{3\,10}P_{10\,13} + r_{3\,11}P_{11\,13} + r_{3\,12}P_{12\,13}$$

$$r_{4\,13} = r_{1\,4}P_{1\,13} + r_{2\,4}P_{2\,13} + r_{3\,4}P_{3\,13} + P_{4\,13} + r_{4\,5}P_{5\,13} + r_{4\,6}P_{6\,13} + r_{4\,7}P_{7\,13} + r_{4\,8}P_{8\,13} + r_{4\,9}P_{9\,13} + r_{4\,10}P_{10\,13} + r_{4\,11}P_{11\,13} + r_{4\,12}P_{12\,13}$$

$$r_{5\,13} = r_{1\,5}P_{1\,13} + r_{2\,5}P_{2\,13} + r_{3\,5}P_{3\,13} + r_{4\,5}P_{4\,13} + P_{5\,13} + r_{5\,6}P_{6\,13} + r_{5\,7}P_{7\,13} + r_{5\,8}P_{8\,13} + r_{5\,9}P_{9\,13} + r_{5\,10}P_{10\,13} + r_{5\,11}P_{11\,13} + r_{5\,12}P_{12\,13}$$

$$r_{6\,13} = r_{1\,6}P_{1\,13} + r_{2\,6}P_{2\,13} + r_{3\,6}P_{3\,13} + r_{4\,6}P_{4\,13} + r_{5\,6}P_{5\,13} + P_{6\,13} + r_{6\,7}P_{7\,13} + r_{6\,8}P_{8\,13} + r_{6\,9}P_{9\,13} + r_{6\,10}P_{10\,13} + r_{6\,11}P_{11\,13} + r_{6\,12}P_{12\,13}$$

$r_{7\,13} = r_{1\,7}P_{1\,13} + r_{2\,7}P_{2\,13} + r_{3\,7}P_{3\,13} + r_{4\,7}P_{4\,13} + r_{5\,7}P_{5\,13} + r_{6\,7}P_{6\,13} + P_{7\,13} + r_{7\,8}P_{8\,13} + r_{7\,9}P_{9\,13} + r_{7\,10}P_{10\,13} + r_{7\,11}P_{11\,13} + r_{7\,12}P_{12\,13}$

$r_{8\,13} = r_{1\,8}P_{1\,13} + r_{2\,8}P_{2\,13} + r_{3\,8}P_{3\,13} + r_{4\,8}P_{4\,13} + r_{5\,8}P_{5\,13} + r_{6\,8}P_{6\,13} + r_{7\,8}P_{7\,13} + P_{8\,13} + r_{8\,9}P_{9\,13} + r_{8\,10}P_{10\,13} + r_{8\,11}P_{11\,13} + r_{8\,12}P_{12\,13}$

$r_{9\,13} = r_{1\,9}P_{1\,13} + r_{2\,9}P_{2\,13} + r_{3\,9}P_{3\,13} + r_{4\,9}P_{4\,13} + r_{5\,9}P_{5\,13} + r_{6\,9}P_{6\,13} + r_{7\,9}P_{7\,13} + r_{8\,9}P_{8\,13} + P_{9\,13} + r_{9\,10}P_{10\,13} + r_{9\,11}P_{11\,13} + r_{9\,12}P_{12\,13}$

$r_{10\,13} = r_{1\,10}P_{1\,13} + r_{2\,10}P_{2\,13} + r_{3\,10}P_{3\,13} + r_{4\,10}P_{4\,13} + r_{5\,10}P_{5\,13} + r_{6\,10}P_{6\,13} + r_{7\,10}P_{7\,13} + r_{8\,10}P_{8\,13} + r_{9\,10}P_{9\,13} + P_{10\,13} + r_{10\,11}P_{11\,13} + r_{10\,12}P_{12\,13}$

$r_{11\,13} = r_{1\,11}P_{1\,13} + r_{2\,11}P_{2\,13} + r_{3\,11}P_{3\,13} + r_{4\,11}P_{4\,13} + r_{5\,11}P_{5\,13} + r_{6\,11}P_{6\,13} + r_{7\,11}P_{7\,13} + r_{8\,11}P_{8\,13} + r_{9\,11}P_{9\,13} + r_{10\,11}P_{10\,13} + P_{11\,13} + r_{11\,12}P_{12\,13}$

$r_{12\,13} = r_{1\,12}P_{1\,13} + r_{2\,12}P_{2\,13} + r_{3\,12}P_{3\,13} + r_{4\,12}P_{4\,13} + r_{5\,12}P_{5\,13} + r_{6\,12}P_{6\,13} + r_{7\,12}P_{7\,13} + r_{8\,12}P_{8\,13} + r_{9\,12}P_{9\,13} + r_{10\,12}P_{10\,13} + r_{11\,12}P_{11\,13} + P_{12\,13}$

where: r_{ij} represents correlation coefficient between the i^{th} and j^{th} trait (i = 1 to 12 and j = 2 to 13) and P_{i13} represents direct effect of the i^{th} trait on trait number 13.

3. Results

The phenotypic correlation coefficients among fourteen vegetative and fruit characters of the nine cacao hybrids are presented in Table 3. Plant height was positively and significantly correlated with stem diameter (0.83), tree circumference (0.60), presence of fruits (0.46), fruit width (0.41) and pod index (0.56), but negatively correlated with time to fruit harvest (–0.47). Time to jorquette was positively (P≤0.05) correlated with time to fruit harvest, (0.43) and fruit weight (0.53) but negatively correlated with pod index (–0.40). Presence of fruit was positively significantly correlated with cherelle wilt (0.57) and pod thickness (0.96). Cherelle wilt was positively significantly correlated with pod thickness (0.55). Time to fruit harvest was positively significantly correlated with fruit weight (0.41), fruit length (0.71), but negatively correlated with fruit width (–0.91) and pod index (–0.83). Number of beans per row was negatively correlated with pod index (–0.71).

The genotypic correlation coefficients among fourteen vegetative and fruit characters of the nine cacao hybrids are presented in Table 4. Plant height was positively significantly (P≤0.01) correlated with stem diameter (2.84), time to jorquette (1.29), tree circumference (2.29), presence of fruit (2.24), fruit width (27.68), pod thickness (19.82), and pod index (4.27) but negatively correlated with number of leaves (–1.62), jorquette height (–1.06),

Table 3. Phenotypic correlation coefficients among fourteen vegetative and fruit characters of nine cacao hybrids used in the study

Character	S D	N L	TTJ	JH	TC	FRT	WLT	TFH	Frt Wt	Frt Lt	Frt Wth	P T	Rows	P. I.
P H	0.83**	0.25	0.10	0.21	0.60**	0.46*	–0.06	–0.47**	–0.09	–0.27	0.41*	0.36	–0.01	0.56**
S D		0.40*	–0.09	0.37*	0.55**	–0.06	–0.41*	–0.45*	–0.01	–0.09	0.48**	–0.17	–0.05	0.36
N L			–0.17	0.09	0.35	–0.09	–0.16	–0.09	–0.23	0.05	0.13	–0.18	0.33	0.06
TTJ				0.11	–0.10	0.25	0.30	0.43*	0.53**	0.29	–0.69**	0.30	–0.27	–0.40*
JH					0.14	–0.32	–0.28	–0.36	0.19	–0.07	0.27	–0.33	–0.30	0.09
TC						0.23	0.01	–0.25	–0.05	–0.08	0.30	0.15	–0.08	0.29
FRT							0.57**	0.03	–0.15	–0.26	–0.10	0.96**	0.25	0.25
WLT								0.30	0.21	–0.15	–0.32	0.55**	0.01	–0.12
TFH									0.41*	0.71**	–0.91**	0.10	–0.05	–0.83**
Frt Wt										0.18	–0.35	–0.17	–0.64**	–0.62**
Frt Lt											–0.66**	–0.11	–0.29	–0.63**
Frt Wth												–0.19	0.04	0.73**
P T													0.14	0.21
Rows														0.15
Bns/Row														–0.71**

NB: df= 25; * and ** = Significance at 0.05 and 0.01 respectively. The values without asterisk are not significant

PH= Plant Height; SD= Stem Diameter; NL= Number of Leaves; TTJ= Time to Jorquette; JH=jorquette Height; TC= Tree Circumference; FRT= Presence of Fruit; WLT= Cherelle Wilt; TFH= Time to fruit harvest; Frt Wt= Fruit Weight; Frt Lt= Fruit Length; Frt Wth = Fruit Width; PT= Pod Thickness; Bns/Row= Number of Beans per row; P. I. = Pod Index

cherelle wilt (–4.09), time to fruit harvest (–2.19), fruit weight (–1.07), fruit length (–0.47) and number of rows (–0.82). Time to jorquette was also highly significantly (P≤0.01) correlated with the rest of the characters except jorquette height. The highly significant correlations of time to jorquette with these characters was however negative with fruit width (–9.98), number of rows (–0.53) and pod index (–0.99). Jorquette height was significantly (P≤0.05) correlated with the rest of the characters except fruit weight, fruit length and pod thickness. The highly significant correlations of jorquette height with these characters was however negative with presence of fruit (–0.68), Cherelle wilt (–1.42), time to fruit harvest (–0.41) and number of rows (–0.41). Tree circumference was positively significantly (P≤0.01) correlated with fruit width (7.96), pod thickness (1.84) and pod index (0.72) but negatively correlated with cherelle wilt (–1.27), time to fruit harvest (-0.42) and number of rows (–0.37). Presence of fruit was positively significantly (P≤0.01) correlated with cherelle wilt (0.57), pod thickness (10.60), and pod index (0.47) but negatively correlated with fruit length (–0.47). Cherelle wilt was also positively significantly (P≤0.01) correlated with time to fruit harvest (0.54), pod thickness (9.52) and pod index (0.54) but negatively correlated with fruit width (–3.76). The correlation of pod index was negative with each of time to fruit harvest (–1.09), fruit weight (–0.75), fruit length (–0.92) and number of beans per row (–0.56). Fruit width was positively correlated with pod index (12.26).

The environmental correlation coefficients among fourteen vegetative and fruit characters of the hybrids are presented in Table 5. Plant height showed positively significant (P≤0.05) correlations with stem diameter (0.65), number of leaves (0.63), jorquette height (0.54), tree circumference (0.42) and cherelle wilt (0.60). Stem diameter showed positively significant (P≤0.05) correlations with number of leaves (1.13), tree circumference (0.98) and cherelle wilt (0.64). Time to jorquette was negatively significantly (P≤0.01) correlated with tree circumference (–0.86) and cherelle wilt (–0.44). Jorquette height was positively significantly correlated with cherelle wilt (0.73) but negatively correlated with time to fruit harvest (–0.55). Tree circumference had positively significant correlations only with the presence of fruit (0.37) and cherelle wilt (0.91). Presence of fruits had positively significant correlation only with cherelle wilt (0.63), but a negative correlation with pod thickness (–0.92). Cherelle wilt was positively significantly (P≤0.01) correlated with the number of rows (0.40) but negative correlations with pod thickness (–0.58) and pod index (–0.79). Time to fruit harvest was negatively significantly correlated with number of rows (–0.43). Fruit weight was negatively correlated with number of rows (–0.78). Fruit width and number of beans per row were negatively significant with pod index (–0.39 and –0.90 respectively).

Table 4. Genotypic correlation coefficients among fourteen vegetative and fruit characters of nine cacao hybrids used in the study

Character	S D	N L	TTJ	JH	TC	FRT	WLT	TFH	Frt Wt	Frt Lt	Frt Wth	P T	Rows	P. I.
P H	2.84**	–1.62**	1.29**	–1.06**	2.29**	2.24**	–4.09**	–2.19**	–1.07**	–0.47**	27.68**	19.82**	–0.82**	4.27**
S D		–0.93**	0.49**	0.70**	–0.23	–0.49**	–2.51**	–0.90**	–0.02	0.27	14.46**	0.88**	–0.48**	0.96**
N L			0.11	0.42	–0.72**	–0.52	–1.34**	–0.25	–0.46*	0.21	5.06**	1.13**	0.42*	0.24
TTJ				0.15	1.25**	0.84**	1.70**	0.78**	1.21**	0.56**	–9.98**	2.39**	–0.53**	–0.99**
JH					0.75**	–0.68**	–1.42**	–0.41*	0.15	0.09	1.57**	0.12	–0.41*	0.78*
TC						0.14	–1.27**	–0.42**	–0.08	–0.14	7.96**	1.84**	–0.37*	0.72*
FRT							0.57*	0.03	–0.25	–0.47**	–0.05	10.60**	0.30	0.47**
WLT								0.54**	0.31	–0.28	–3.76**	9.52**	–0.33	0.54**
TFH									0.44*	0.89**	–9.17**	0.66**	–0.02	–1.09**
Frt Wt										0.24	–4.85**	–0.42	–0.61**	–0.75*
Frt Lt											–9.89**	–1.21**	–0.30	–0.92**
Frt Wth												–17.20**	2.56**	12.26**
P T													1.37**	0.38
Rows														0.11
Bns/Row														–0.56**

NB: df= 25; * and ** = Significance at 0.05 and 0.01 respectively. The values without asterisk are not significant

PH= Plant Height; SD= Stem Diameter; NL= Number of Leaves; TTJ= Time to Jorquette; JH=jorquette Height; TC= Tree Circumference; FRT= Presence of Fruit; WLT= Cherelle Wilt; TFH= Time to fruit harvest; Frt Wt= Fruit Weight; Frt Lt= Fruit Length; Frt Wth = Fruit Width; PT= Pod Thickness; Bns/Row= Number of Beans per row; P. I. = Pod Index

Table 5. Environmental correlation coefficients among fourteen vegetative and fruit characters of nine cacao hybrids used in the study

Character	S D	N L	TTJ	JH	TC	FRT	WLT	TFH	Frt Wt	Frt Lt	Frt Wth	P T	Rows	P. I.
P H	0.65**	0.63**	–0.04	0.54**	0.42*	0.18	0.60**	–0.25	0.24	–0.32	–0.15	–0.29	0.22	–0.16
S D		1.13**	–0.32	0.17	0.98**	0.33	0.64**	0.13	0.00	–0.38	–0.35	–0.30	0.33	–0.07
N L			–0.33	–0.22	1.17**	0.48**	0.69**	0.61**	0.15	–0.14	–0.29	–0.41	0.24	–0.14
TTJ				0.09	–0.86**	–0.28	–0.44**	0.06	–0.18	0.09	–0.17	0.10	–0.06	0.04
JH					–0.44	0.26	0.73**	–0.55**	0.33	–0.29	0.22	–0.51	–0.14	–0.84
TC						0.37*	0.91**	0.16	0.01	–0.02	–0.30	–0.06	0.30	–0.16
FRT							0.63**	0.11	0.16	0.13	–0.18	–0.92**	0.12	–0.14
WLT								–0.31	0.09	–0.03	–0.10	–0.58**	0.40*	–0.79**
TFH									0.29	0.22	0.09	–0.07	–0.43*	0.02
Frt Wt										0.02	0.23	–0.27	–0.78**	–0.35
Frt Lt											0.22	0.07	–0.27	–0.17
Frt Wth												0.10	–0.31	–0.39*
P T													–0.09	0.26
Rows														0.24
Bns/Row														–0.90**

NB: df= 25; * and ** = Significance at 0.05 and 0.01 respectively. The values without asterisk are not significant
PH= Plant Height; SD= Stem Diameter; NL= Number of Leaves; TTJ= Time to Jorquette; JH=jorquette Height; TC= Tree Circumference; FRT= Presence of Fruit; WLT= Cherelle Wilt; TFH= Time to fruit harvest; Frt Wt= Fruit Weight; Frt Lt= Fruit Length; Frt Wth = Fruit Width; PT= Pod Thickness; Bns/Row= Number of Beans per row; P. I. = Pod Index

The direct and indirect path coefficients that estimate the strength of the relationship between pod index and the vegetative and fruit characters using the genotypic correlation values is presented in table 6. Fruit length had the largest positive direct effect (4.5487) on pod index, with its largest indirect effect through time to jorquette (1.6755). The largest negative indirect effect of fruit length on pod index is through time to fruit harvest (–7.5772). Cherelle wilt also had a notably large positive direct effect (3.5830) 0n pod index, with its largest indirect effect also through time to jorquette (5.0864). The largest negative indirect effect of cherelle wilt on pod index is through time to fruit harvest (–4.5974). Time to fruit harvest had the largest negative direct effect (–8.5137) on pod index, with its largest indirect effect through fruit length (4.0484). The negative direct effects of jorquette height (–0.4375), and plant height (–0.2087) on pod index are also noteworthy. Jorquette height had its largest indirect effect also through time to fruit harvest (3.4906). Though the number of characters used in the path coefficient analysis was large, the residual factor was 1.7558.

Table 6. Direct and indirect path coefficients between pod index and twelve vegetative and fruit characters of nine cacao hybrids

		Indirect effects through other plant characters											
	Direct effect	PH	SD	TTJ	JH	TC	FRT	WLT	TFH	Frt Wt	Frt Lt	Frt Wth	Bns/Row	Corr with Pod index
PH	**–0.2087**		1.4382	3.8597	0.4637	0.6822	–6.3551	–14.6547	18.645	4.4176	–2.1379	–2.7851	0.9052	4.27
SD	**0.5064**	–0.5928		1.4661	–0.3062	–0.0685	1.3902	–8.9934	7.6623	0.0826	1.2282	–1.4549	0.0402	0.96
TTJ	**2.992**	–0.2693	0.2481		–0.0656	0.3724	–2.3832	6.0912	–6.6407	–4.9956	2.5473	1.0042	0.1092	–0.99
JH	**–0.4375**	0.2212	0.3545	0.4488		0.2234	1.9292	–5.0879	3.4906	–0.6193	0.4094	–0.158	0.0055	0.78
TC	**0.2979**	–0.4780	–0.1165	3.7400	–0.3281		–0.3972	–4.5505	3.5758	0.3303	–0.6368	–0.8009	0.084	0.72
FRT	**–2.8371**	–0.4675	–0.2481	2.5133	0.2975	0.0417		2.0423	–0.2554	1.0321	–2.1379	0.005	0.4841	0.47
WLT	**3.583**	0.8537	–1.2711	5.0864	0.6212	–0.3783	–1.6171		–4.5974	–1.2799	–1.2736	0.3783	0.4348	0.54
TFH	**–8.5137**	0.4571	–0.4558	2.3338	0.1794	–0.1251	–0.0851	1.9348		–1.8166	4.0484	0.9227	0.0301	–1.09
Frt Wt	**–4.1286**	0.2233	–0.0101	3.6203	–0.0656	–0.0238	0.7093	1.1107	–3.7460		1.0917	0.4880	–0.0192	–0.75
Frt Lt	**4.5487**	0.0981	0.1367	1.6755	–0.0394	–0.0417	1.3334	–1.0033	–7.5772	–0.9909		0.9951	–0.0553	–0.92
Frt Wth	**–0.1006**	–5.7774	7.3226	–29.8601	–0.6868	2.3711	0.1419	–13.4723	78.0706	20.0236	–44.987		–0.7855	12.26
Bns/Row	**0.0457**	–4.1369	0.4456	7.1509	–0.0525	0.5481	–30.0732	34.1106	–5.619	1.734	–5.504	1.7306		–0.56

PH= Plant Height; SD= Stem Diameter; TTJ= Time to Jorquette; JH=jorquette Height; TC= Tree Circumference; FRT= Presence of Fruit; WLT= Cherelle Wilt; TFH= Time to fruit harvest; Frt Wt= Fruit Weight; Frt Lt= Fruit Length; Frt Wth= Fruit Width; Bns/Row= Number of Beans per row
Residual effect = 1.7558

4. Discussion

The mutual association among characters is often expressed by the phenotypic, genotypic and environmental correlations [8,9]. Phenotypic correlation is a composite of genotypic and environmental correlations. In this study, the genotypic correlation coefficients were in most cases higher than the corresponding phenotypic correlation coefficients and the environmental correlation coefficients. This has been ascribed to reduced values of environmental correlations between the corresponding characters implying reduced influence by the environment [8]. This implies that the genotypic factor had a greater contribution in the development of the character association [10]. The low values of the environmental correlation coefficients imply that the phenotypic correlation coefficients would be good indicators of genotypic correlation coefficients. This is supported by the findings of Kalambe *et al* on cowpea [11].

Selection of the genotypes based only on inter-character associations which are genotypically correlated but not phenotypically correlated may not be of practical value since selection is mostly based on the phenotypes of the characters. Such a selection will be unrepeatable and unreliable [1]. This applies to the pairs of characters that exhibited this kind of relationship in the study, such as stem diameter, fruiting and wilted fruits with pod index.

The significant genotypic and phenotypic correlations of many of the pairs of the vegetative and fruit characters with one another and with pod index suggested that these characters contributed either positively or negatively to growth and yield in the cacao genotypes. Such inter-character associations can therefore be used as criteria for selection of the genotypes that particularly exhibit good yield. This relationship applies to plant height, time to jorquette, time to fruit harvest, fruit length and fruit width with pod index. Significant correlations of yield-related characters in young cacao plants were reported by Santos *et al.* [12].

The direct and indirect relationships between pod index and the vegetative and fruit characters of the nine cacao genotypes indicated that plant height, jorquette height, fruiting, time to fruit harvest, fruit weight and fruit width all had a negative direct effects on pod index. These relationships are very desirable. It implies that an inverse relationship exists between each of these traits and pod index, i.e. an increase in the value of each of these results in a corresponding reduction in the pod index. Since pod index refers to the number of cocoa pods required to produce 1.0 kg of dry cocoa beans [13], the lower the value, the more desirable the genotype. Any character whose incremental value will reduce the numerical value of pod index is therefore of utmost importance. Thondaiman and Rajamani [14] reported similar findings in cacao.

The valuable negative indirect effects of these plant traits on pod index include their effects through fruiting, cherelle wilt, fruit length and fruit width (for plant height); fruit wilt, fruit weight and fruit width (for jorquette height); plant height, stem diameter, time to fruit harvest and fruit length (for fruiting); stem diameter, tree circumference, fruiting and fruit weight (for time to fruit harvest); stem diameter, jorquette height, tree circumference, time to fruit harvest and pod thickness (for fruit weight); and plant height, time to jorquette, cherelle wilt, fruit length and pod thickness (for fruit width). Each of plant height, jorquette height, fruiting, time to fruit harvest, fruit weight and fruit width can therefore be considered along with any or all of each of the other traits that enhance their negative expression in the screening or selection of these cacao genotypes for desirable pod index. Initial increase in the tree circumference can result in better yield (pod index), when tree circumference is considered in association with jorquette height, fruiting, cherelle wilt, fruit length and fruit width, which all had negative indirect correlations with pod index. The other traits such as stem diameter, time to jorquette, cherelle wilt, fruit length and pod thickness which had positive direct effect on pod index (which is not desirable in this context) can also be considered in conjunction with the traits which had negative indirect effect on pod index. Thondaiman and Rajamani [14] also reported findings similar to these. The significant value of the residual factor in spite of the large number of characters used in the path coefficient analysis may be due to the fact that correlations are mere estimates, and may also be due to rounding-off errors.

5. Conclusions

Significant association existed among most traits under consideration, and such traits significantly determined yield as indicated by pod index in cacao. These traits, therefore, are important for consideration in further yield improvement procedures in cacao.

Conflict of Interest

There exists no conflict of interest with respect to the entire process leading to the submission of this article for publication.

References

[1] Adenuga, O.O., Adepoju, A.F., Olaniyi, O.O., et al., 2018. Relationships among bean yield traits in some Cacao (*Theobroma cacao* L.) genotypes. Journal of

Agricultural Science and Technology B. 8(5), 303-310.

[2] Goenaga, R., Guiltinan, M., Maximova, S., 2018. Yield Performance and Bean Quality Traits of Cacao Propagated by Grafting and Somatic Embryo-derived Cuttings. American Society for Horticultural Science.

[3] John, K., Madhavi Santhoshi, M.V., Rajasekhar, P., 2019. Correlation and path analysis in groundnut (*Arachis hypogaea* L). International Journal of Current Microbiology and Applied Sciences. 8(12), 1521-1529.

[4] Falconer, D.S., 1989. Introduction to Qualitative Genetics. 2nd edition. Longman. London. pp. 340.

[5] Miller, P.A., Williams, V.C., Robinson, H.P., et al., 1958. Estimates of Genotype and Environmental Variances and Covariances in Upland Cotton and Their Implications in Selection. Agronomy Journal. 50, 126-131.

[6] Lowry, R., 2009. Appendix to chapter 4: The significance of a correlation coefficient. http://faculty.vassar.edu/lowry/chaapx.html. (28 December 2009). London, UK. pp. 22.

[7] Dewey, L.R., Lu, K.H., 1957. A correlation and path analysis of crested heat grass seed production. Agronomy Journal. 51, 515-518.

[8] Searle, S.R., 1961. African indigenous vegetables: An overview of the cultivated species. Chatham., UK. pp. 89-98.

[9] Ariyo, O.J., 1989. Variation and heritability of fifteen characters in okra (*Abelmoschus esculentus* (L.) Moench). Tropical Agricultural Journal (Trinidad). 67, 215-216.

[10] Arshad, M., Ali, N., Ghafoor, A., 2006. Character correlation and path coefficient in soybean *glycine max* (1.) Merrill. Pakistan Journal of Botany. 38, 121-130.

[11] Kalambe, A.S., Wankdade, M.P., Deshmakh, J.D., et al., 2019. Correlation studies in cowpea (*Vigna unguiculata* L.). Journal of Pharmacognosy and Phytochemistry. 8(3), 321-323

[12] Santos, E.A.D., Almeida, A.A.F.D., Branco, M.C.D.S., et al., 2018. Path analysis of phenotypic traits in young cacao plants under drought conditions. PloS ONE. 13(2), e0191847.
DOI: https://doi.org/10.1371/journal.pone.0191847

[13] Wood, G.A., Lass, R.A., 1985. Cacao 4th edition, Longman, U.K. pp. 620.

[14] Thondaiman, V., Rajamani, K., 2014. Correlation and path coefficient analysis of yield components in cacao (*Theobroma cacao* L.). Journal of Plantation Crops. 42(3), 358-363.

BILINGUAL PUBLISHING CO.
Pioneer of Global Academics Since 1984

Journal of Botanical Research
https://ojs.bilpublishing.com/index.php/jbr

ARTICLE

Terpenes of the Essential Oil from *Ipomoea alba* Leaf in Response to Herbivore and Mechanical Injuries

José L. S. de Almeida Clécio S. Ramos*

Department of Chemistry, Rural Federal University of Pernambuco, 52.171-030, Recife-Pe, Brazil

ARTICLE INFO

Article history
Received: 6 May 2022
Revised: 21 June 2022
Accepted: 23 June 2022
Published Online: 7 July 2022

Keywords:
Elaeochlora trilineata
Ipomoea alba
Grasshopper
Germacrene D
Terpenes
Herbivory

ABSTRACT

There is no doubt that the chemical composition of plants, including nor-volatile and volatile compounds, is widely affected by abiotic and biotic stress. Plants are able to biosynthesize a variety of secondary metabolites against actions of natural enemies, such as herbivores, fungus, virus and bacteria. The present study revealed that the chemical compositions of leaf essential oils from *Ipomoea alba* underwent quantitative and qualitative alterations both when infested with the grasshopper *Elaeochlora trilineata* and mechanically damaged. Grasshopper attack and mechanical wounding induced the biosynthesis of nine volatile compounds in leaves of *I. alba*: cumene, *α*-ylangene, *β*-panasinsene, *β*-gurjunene aromadendrene, *β*-funebrene, spirolepechinene, cubenol and sclareolide. The amount of germacrene D (33.2% to 20.4%) decreased when the leaves were mechanically damaged; but when the leaves were attacked by a grasshopper, the germacrene D increased from 33.2% to 39.4%. The results showed that *I. alba* leaves clearly responded to abiotic and biotic stress and contribute to an understanding of plant responses to stress conditions.

1. Introduction

The chemical composition of plants can vary greatly in response to abiotic and biotic stress, such as soil salinity, temperature, humidity and nutrient deficiency, pathogen infection and herbivore attack [1,2]. In particular, plants biosynthesize a wide spectrum of secondary metabolites when they are injured by herbivores, including volatile compounds that consist predominantly of terpenes and widely known as allelochemicals [3,4].

Terpenes represent the main and most abundant class of plant secondary compounds, with approximately 55,000 elucidated chemical structures. Volatile terpenes are associated with abiotic and biotic stress tolerance [5,6]. Monoterpene linalool and sesquiterpene (*E*)-*β*-farnesene, biosynthesized by plants, act as allomones in herbivores and aphids, respectively [7]. Terpenes (-)-*α*-bisabolol, carvacrol, (+)-terpinen-4-ol and thymol are active against the Colorado potato beetle (*Leptinotarsa decemlineata*), whereas terpenes (-)-verbenone, camphor and linalyl

*Corresponding Author:
Clécio S. Ramos,
Department of Chemistry, Rural Federal University of Pernambuco, 52.171-030, Recife-Pe, Brazil;
Email: clecio.ramos@ufrpe.com

DOI: https://doi.org/10.30564/jbr.v4i3.4699

acetate have shown antifeedant activities [8]. *Chelonus insularis*, a wasp egg-larval endoparasitoid, is attracted to a blend of terpenes α-pinene, α-longipinene and α-copaene emitted by maize plants, mainly when the plant is damaged by *Spodoptera frugiperda* larvae [9].

Our previous studies showed that other classes of secondary metabolites, such as phenylpropanoids, have been related to the induced response of plants to biotic and abiotic stress. For example; Phenylpropanoids myristicin, dilapiol, eugenol and eugenol acetate were only identified in the essential oil of *Mangifera indica* leaves damaged by the grasshopper *Tropidacris Collaris* and mechanically [10]. Phenylpropanoid dillapiole has been previously reported in the essential oil of the *Solanum paniculatum* leaf as the plant's chemical defense to abiotic stress [11]. Biotic and abiotic stress can also affect the biological potential of plants as in the case of *Piper marginatum* leaves: *P. marginatum* essential oil obtained from the leaves damaged by insects showed lower antimicrobial potential against fungi and bacteria when compared to essential oil obtained from healthy leaves [12].

In our ongoing study to identify compounds associated with plant chemical defense [13], here we describe changes in the chemical profile of essential oils obtained from *Ipomoea alba* L. leaves after a grasshopper (*Elaeochlora trilineata*) attack or by mechanical injury. *I. alba*, popularly known as the moonflower or moonvine, is native to the Caribbean, Mexico and Brazil, where the plant is used in folk medicine due to its purgative, analgesic, anti-inflammatory, anti-rheumatism, antimicrobial, anti-pyretic, hypotensive and emollient properties [14,15].

There are few reports on chemical studies of *I. alba.* Indolizine alkaloids and glycoside have previously been isolated from *I. alba* seeds [16,17]. In relation to studies on the chemistry of the essential oils from the *I. alba* leaf on the biotic and abiotic stress, to our knowledge there are no reports.

2. Material and Method

2.1 Plant and Insect

Fresh leaves from *I. alba* were collected on Campus of Federal Rural University of Pernambuco (UFRPE) to obtain their essential oils. The plant was identified by Dr. Margareth F. de Sales of the same university and a voucher of species was deposited at the Vasconcelos Sobrinho Herbarium of the Federal Rural University of Pernambuco, Recife city, Brazil. Adult grasshoppers of the *species Elaeochlora trilineata* were collected on the campus of UFRPE and identified by Dr Argus Vasconcelos de Almeida (Department of Biology, UFRPE).

2.2 Stress Conditions

Adult *I. alba* stems with undamaged and insect-free leaves were collected from specimens (N = 3) growing on the campus of the Federal Rural University of Pernambuco (Figure 1) and maintained for 24 h in bottles with water in a greenhouse without supplementary lighting. Collected leaves (3 bottles) were infested during 4 hours with the *E. trilineata* grasshopper (10 specimens to each sample) to simulate biotic stress. Mechanical damage was caused by piercing leaf tissues (3 bottles) with a paper punch to simulate abiotic stress over a period of 4 h. Five 80 mm holes were punched in each leaf. Plant samples (N = 3) with healthy and undamaged leaves were collected and used as negative control.

Figure 1. *I. alba* leaves healthy and submitted to abiotic and biotic stress.

2.3 Essential Oil Extraction

The essential oils from the undamaged leaves of the *I. alba* as well as those under biotic and abiotic stress (400 g each), were extracted using a modified Clevenger-type apparatus and subject to hydrodistillation for 2 h. The oil layers were separated and dried over anhydrous sodium sulfate, stored in hermetically sealed glass containers, and kept under refrigeration at 5 ºC until analysis. All experiments were carried out in triplicate.

2.4 Quantitative Analysis of Essential Oils

Analysis by gas chromatography (GC) was performed in a Hewlett Packard 5890 Series II GC machine equipped with a flame ionization detector (FID) and a non-polar DB-5 fused silica capillary column (30 m × 0.25 mm × 0.25 µm film thickness). The oven temperature was programmed to rise from 50 °C to 250 °C at a rate 3 C/min for integration purposes. Injector and detector temperatures were 250 °C. H_2 was used as the carrier gas at a flow rate of 1 L/min and 30 psi. inlet pressure in split mode (1:20). The injection volume was 1.0 µL of dilution solution (1/100) of oil in hexane. The relative concentrations of the identified constituents were calculated by base of the GC peak areas in the order of DB-5 column elution and expressed as a relative percentage of the total area of all the peaks. All the oil samples were analyzed in triplicate.

2.5 Chemical Identification of Essential Oils

The essential oils were analysed by gas chromatography/mass spectrometry (GC/MS) (50-250 ºC at 3 ºC min. rate) using a Hewlett-Packard GC/MS system (CG:5890 Series II/CG–MS: MSD 5971) equipped with a fused-silica capillary column (30 m × 0.25 mm i.d. × 0.25 µm) coated with DB-5column. The injector and detector temperatures were 250 °C and 260 °C, respectively. MS spectra were obtained using electron impact at 70 eV with a scan interval of 0.5 s, fragments from 40 Da to 550 Da, He carrier gas, flow rate 1 mL/min, split mode (1:20), injection volume 1 µL of dilution solution (1/100) of oil in hexane. Compound identification was established in retention indices with reference to a homologous series of C11–C24 n-alkanes, calculated using the Van den Dool and Kratz equation and by comparison with the GC/MS library mass spectra acquired from the data system [18,19].

3. Results and Discussion

The chromatograms obtained by GC/MS of essential oil samples from healthy and damaged leaves of *I. alba* showed qualitative and quantitative differences when compared to each other (Figure 2). Previous studies have revealed that the chemical composition of essential oils from *Ipomoea* species is constituted mainly of sesquiterpenes such as germacrene, cis-cadin-1(6),4-diene, humulene, caryophyllene, copaene, bicyclogermacrene, cadinol and murolene [20]. To our knowledge, there has been only one study on the chemistry of the essential oil from *I. alba* leaves, where the major constituent was identified as germacrene D (leaves 27.8% and flowers 45.8%) [20].

It was possible to identify sixteen compounds: four terpenes: *δ*-elemene, *E*-caryophyllene, germacrene D and c*is*-cadina-1,4-diene were found in the three oils. Sesquiterpene germacrene D was identified as the major compound with 39.4%, for leaves under biotic stress; 20.4%, for leaves under abiotic stress, and 33.2%, for healthy leaves (Table 1). Terpenes represent the largest and structurally the most diverse group of volatiles released by plants and are emitted either constitutively or induced in response to abiotic and biotic stresses [21]. Germacrene D commonly occurs in plants and has been identified in angiosperms, gymnosperms and bryophytes. Germacrene D is a precursor of various sesquiterpenes and it has been reported to have repellent and insecticidal activity [22]. For example, germacrene D has been

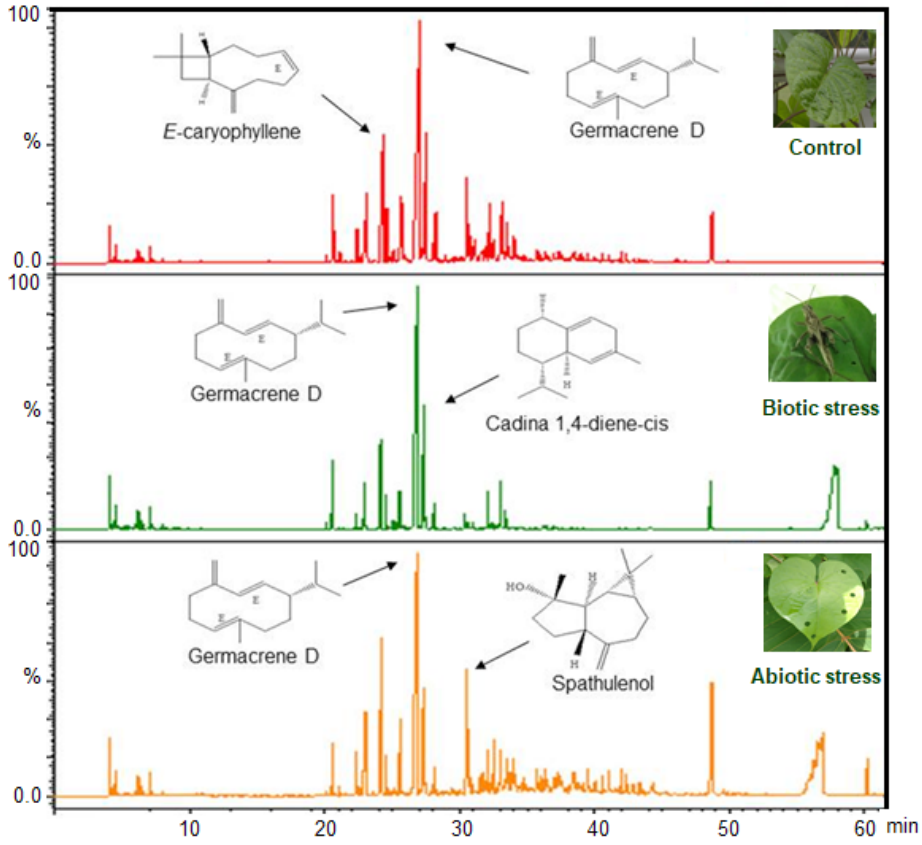

Figure 2. Chromatograms obtained by GC/MS of essential oils from *I. alba* leaves: healthy (Control) and damaged (Biotic and abiotic stress)

reported to have mosquitocidal activity against three mosquito species, *Anopheles gambiae*, *Culex quinquefasciatus* and *Aedes aegypti* [23].

Here, a total of nine volatile organic compounds have been identified in response to biotic and abiotic stress: cumene, *α*-ylangene, *β*-panasinsene, *β*-gurjunene aromadendrene, *β*-funebrene, spirolepechinene, cubenol and sclareolide.

In the essential oil from the biotic-stressed, herbivore-damaged leaf, the presence of only two compounds has been identified that had not been found in the essential oil samples from undamaged or mechanically-damaged leaves: *β*-Gurjunene (2.1%) and spirolepechinene (2.5%), associated with the inducible defense of *I. alba* in response to damage by the grasshopper *E. trilineata*. Essential oil extracted from the *Dipsacus asper* roots exhibited larvicidal activity against *Aedes aegypti* and *Culex pipiens; β*-Gurjunene has been identified as one of the major compounds in the oil [24]. The spirolepechinene is a spirosesquiterpene found in *Lepechinia bullata* and of a unique structure [25].

The *β*-funebrene and sclareolide were produced by the leaves of *I. alba* in significant quantities in response to injuries by the grasshopper and by mechanical injury. Sclareolide is a sesquiterpene lactone with antimicrobial and cytotoxic activity. It is derived from various plant sources including *Salvia sclarea* and *Nicotiana tabacum* [26]. *β*-funebrene has been identified as one of the main compounds in the essential oil of *Campomanesia adamantium* leaves, a plant used for its antiinflammatory, anti-diarrhoeal and antimicrobial activities [27].

A great number of compounds have been identified for essential oil from *I. alba* leaves in response to abiotic stress (cumene, *α*-ylangene, *β*-panasinsene, *β*-funebrene, aromadendrene, cubenol and sclareolide). Sesquiterpene *α*-ylangene has been identified in some essential oils of plants with diverse biological activities, but only as a minor compound [28]. Essential oil of *Eucalyptus globulus* has been reported to have insecticidal activity against insecticidal on *Acanthoscelides obtectus* adults as well as against the red mite *Dermanyssus gallinae;* some terpenes, including aromadendrene, have been associated with

Table 1. Chemical constituents of essential oils from healthy (Control) and damaged (Abiotic and biotic stress) *I. alba* leaves

Compounds	RI[a]	RI[b]	Essential oils (%)[c]		
			Control	Abiotic	Biotic
1.Cumene	993	924		0.7± 0.02	1.1 ± 0.01
2.*δ*-Elemene	1331	1335	4.2 ± 0.01	0.7 ± 0.00	4.7± 0.01
3.α-Ylangene	1372	1373		1.7 ± 0.02	
4.*β*-Panasinsene	1385	1382		1.1 ± 0.03	
5.*β*-Elemene	1389	1389	3.3 ± 0.04	4.0 ± 0.01	
6.*β*-Funebrene	1418	1413		6.3 ± 0.02	6.1 ± 0.02
7.*E*-Caryophyllene	1420	1417	13.6 ± 0.01	5.2 ± 0.02	3.9 ± 0.03
8.*β*-Gurjunene	1428	1431			2.1± 0.04
9.Spirolepechinene	1454	1449	3.7 ± 0.03		
10.Aromadendrene	1453	1458		3.5 ± 0.03	
11.Spirolepechinene	1451	1449			2.5
12.Germacrene D	1482	1484	33.2 ± 0.00	20.4 ± 0.01	39.4 ± 0.01
13.*Cis*-cadina-1,4-diene	1497	1495	10.3 ± 0.02	5.2 ± 0.02	11.8 ± 0.01
14.Spathulenol	1580	1577	4.1 ± 0.02	9.8 ± 0.01	
15.Cubenol	1629	1627		2.3 ± 0.02	
16.Sclareolide	2108	2065		6.7 ± 0.01	3.3 ± 0.02
	Total (%)		72.4 ± 0.01	67.5 ± 0.02	74.8 ± 0.02
	Oil yields (%)		0.19 ± 0.02	0.23 ± 0.01	0.20 ± 0.01

[a]Retention indices calculated from retention times in relation to those of the series n-alkanes on a 30 m DB-5 capillary column. [b]Retention indices from the literature [c]Composition: total area percentages given as mean ± SD (n = 3).

oil activity [29]. The essential oil of the *Blepharocalyx cruckshanksii* leaves with 24.5% of cubenol showed insecticidal, repellent and anti-food activity against the horn fly, *Haematobia irritans*, considered the largest livestock pest in the world [30].

In our study, the main quantitative variations between the essential oils of damaged and healthy leaves consisted among their major compounds. In the healthy leaves, the principal component was identified as germacrene D. This decreased when the leaves suffered mechanical damage. A significant increase in the amount of germacrene D (33.2% to 39.4%) was observed when the leaves were injured by the grasshopper *E. trilineata*.

4. Conclusions

In summary, we identified nine volatiles compounds from essential oils of *I. alba* leaves in response to abiotic and biotic stress. The results obtained contribute significantly to knowledge about plant chemistry under stress conditions, mainly for the genus *Ipomoea*.

Acknowledgments

The authors are indebted to the Centro de Apoio a Pesquisa of the Federal Rural University of Pernambuco (CENAPESQ), for the laboratory facilities. The authors are also grateful to Dr. Margareth F. de Sales for identification of *I. alba* and Dr. Argus V. de Almeida for the identification of grasshopper *E. trilineata.*

Conflict of Interest

No potential conflict of interest was reported by the authors.

References

[1] Morales-Tapia, P., Cabrera-Barjas, G., Giordano, A., 2021. Polyphenolic distribution in organs of *Argylia radiata*, an extremophile plant from Chilean Atacama desert. Natural Product Research. 35, 4143-4147.

[2] Fichman, Y., Mittler, R., 2020. Rapid systemic signaling during abiotic and biotic stresses: is the ROS wave master of all trades? Plant Journal. 102(5), 887-896.

[3] De Lange, E.S., Laplanche, D., Guo, H., et al., 2020. *Spodoptera frugiperda* Caterpillars Suppress Herbivore-Induced volatiles Emissions in Maize. Journal of Chemical Ecology. 46(3), 344-360.

[4] Ulhoa, L.A., Barrigossi, J.A.F., Borges, M., et al., 2020. Differential induction of volatiles in rice plants by two stink bug species influence behaviour of conspecifics and their natural enemy *Telenomus podisi*. Entomologia Experimentalis et Applicata. 168(1), 76-90.

[5] Boncan, D.A.T., Tsang, S.S., Li, C., et al., 2020. Terpenes and terpenoids in plants: Interactions with environment and insects. International Journal of Molecular Sciences. 21(19), 7382.

[6] Schwab, W., Fuchs, C., Huang, F.C., 2013. Transformation of terpenes into fine chemicals. European journal of lipid science and technology. 115(1), 3-8.

[7] Gonzalo, E.C., Raúl, S.V., Isabel, B.M., et al., 2017. Antifeedant effects of common terpenes from Mediterranean aromatic plants on Leptinotarsa decemlineata. Journal of soil science and plant nutrition. 17(2), 475-485.

[8] Sharma, E., Anand, G., Kapoor, R., 2017. Terpenoids in plant and arbuscular mycorrhiza-reinforced defence against herbivorous insects. Annals of Botany. 119(5), 791-801.

[9] Fabian, R., Rojas, J.C., Cisneros, J., et al., 2019. Herbivore-Induced Volatiles from Maize Plants Attract *Chelonus insularis*, an Egg-Larval Parasitoid of the Fall Armyworm Ortiz-Carreon. Journal of Chemical Ecology. 45(3), 326-337.

[10] Silva, R.R., Câmara, C.A.G., Almeida, A.V., et al., 2012. Biotic and abiotic stress-induced phenylpropanoids in leaves of the mango (*Mangifera indica* L., Anacardiaceae). Journal of the Brazilian Chemical Society. 23(2), 206-2011.

[11] Ramos, N.S.M., Ramos, C.S., 2013. Volatiles from *Solanum paniculatum* Leaves in Response to Mechanical Damage. Chemistry of Natural Compounds. 49, 953-954.

[12] Silva, A.S., Silva, M.A., Almeida, A.V., et al., 2016. Herbivory causes chemical and biological changes on essential oil from *Piper marginatum* leaves. The Natural Products Journal. 6, 1-5.

[13] Silva, R.R., Moraes, M.M., Câmara, C.A.G., et al., 2015. Change in the profile chemical of leaves *Mangifera indica* after their metabolism on grasshopper *Tropidacris collaris*. Natural Product Communications. 10, 1809-1810.

[14] Lawson, S.K., Davis, M.N., Brazell, C., et al., 2017. Chloroform extracts of *Ipomoea alba* and *Ipomoea tricolor* Seeds Show Strong in-vitro antibacterial, antifungal, and cytotoxic activity. Journal of Pharmacognosy and Phytochemistry. 6(5), 730-734.

[15] Brasileiro, B.G., Pizziolo, V.R., Raslan, D.S., 2006. Antimicrobial and cytotoxic activities screening of some Brazilian medicinal plants used in Governador Valadares district. Brazilian Journal of Pharmaceutical Sciences. 42, 195-202.

[16] Castaneda-Gomez, J., Rosas-Ramirez, D., Cruz-Morales, S., et al., 2017. HPLC-MS profiling of the multidrug-resistance modifying resin glycoside content of *Ipomoea alba* seeds. Revista Brasileira de Farmacognosia. 27(4), 434-439.

[17] Ikhiri, K., Koulodo, D.D.D., Garba, M., et al., 1987. New indolizine alkaloids from *Ipomoea alba*. Journal of Natural Products. 50(2), 152-156.

[18] Adams, R.P., 2007. Identification of essential oil components by gas chromatography/ quadrupole mass spectroscopy. Allured Publishing Corporation. Carol Stream. Illinois. pp. 468.

[19] Van Den Dool, H., Kratz, P.D., 1963. A Generalization of the Retention Index System Including Linear Temperature Programmed Gas-Liquid Partition Chromatography. Journal of Chromatography A. 11, 463-471.

[20] Tenório, T.M., Moraes, M.M., Camara, C.A., et al., 2021. Scents from the Brazilian Atlantic Forest Biome: chemical composition of essential oils from the leaves and flowers of seven species of *Ipomoea* (Convolvulaceae). Journal of Essential Oil Research. 33(6), 567-583.

[21] Esha Sharma, G.A., Rupam, K., 2017. Terpenoids in plant and arbuscular mycorrhiza-reinforced defence against herbivorous insects. Annals of Botany. 119, 791-801.

[22] Noge, K., Becerra, J.X., 2009. Germacrene D, a common sesquiterpene in the genus *Burser*a (Burseraceae). Molecules. 14(12), 5289-5297.

[23] Ravi Kiran, S., Sita Devi, P., 2007. Evaluation of mosquitocidal activity of essential oil and sesquiterpenes from leaves of *Chloroxylon swietenia* DC. Parasitology research. 101(2), 413-418.

[24] Lu, H.Y., Liu, X.C., Liu, Q.Z., et al., 2017. Chemical composition of *Dipsacus asper* Wallich ex Candolle (Dipsacaceae) essential oil and its activity against mosquito larvae of *Aedes aegypti* and *Culex pipiens* pallens. Tropical Journal of Pharmaceutical Research. 16(1), 179-184.

[25] Chappell, J., O'Maille, P.E., Noel, J.P., 2006. Biosynthetic potential of sesquiterpene synthases: alternative products of tobacco 5-epi-aristolochene synthase. Archives of Biochemistry and Biophysics. 448, 73-82.

[26] Hayet, E., Fatma, B., Souhir, I., et al., 2007. Antibacterial and cytotoxic activity of the acetone extract of the flowers of *Salvia sclarea* and some natural products. Pakistan Journal Pharmaceutical Science. 20, 146-148.

[27] Sá, S., Chaul, L.T., Alves, V.F., et al., 2018. Phytochemistry and antimicrobial activity of Campomanesia adamantium. Revista Brasileira de Farmacognosia. 28, 303-311.

[28] Basile, S., Badalamenti, N., Riccobono, O., et al., 2022. Chemical Composition and Evaluation of Insecticidal Activity of *Calendula incana* subsp. *maritima* and *Laserpitium siler* subsp. *siculum* Essential Oils against Stored Products Pests. Molecules. 27(3), 588.

[29] Hikal, W.M., Baeshen, R.S., Said-Al Ahl, H.A., 2017. Botanical insecticide as simple extractives for pest control. Cogent Biology. 3, 1404274.

[30] Espinoza, J., Medina, C., Aniñir, W., et al., 2021. Insecticidal, Repellent and Antifeedant Activity of Essential Oils from *Blepharocalyx cruckshanksii* (Hook. & Arn.) Nied. Leaves and *Pilgerodendron uviferum* (D. Don) Florin Heartwood against Horn Flies, *Haematobia irritans* (Diptera: Muscidae). Molecules. 26(22), 6936.

BILINGUAL PUBLISHING CO.
Pioneer of Global Academics Since 1984

Journal of Botanical Research
https://ojs.bilpublishing.com/index.php/jbr

ARTICLE

Evaluation of Tung Oil (*Vernicia fordii* (Hemsl.)) for Controlling Termites

Hangtian Li[1] Siying Li[1] Hui Lu[2] Jingjing Zhang[1] Xi Yang[2] Dayu Zhang[2] Yike Zhang[2] Yongjian Xie[2*]

1. Institute of Termite Control of Yuhang, Hangzhou, 311100, China
2. College of Advanced Agricultural Sciences, Zhejiang A&F University, Hangzhou 311300, China

ARTICLE INFO

Article history
Received: 14 June 2022
Revised: 12 July 2022
Accepted: 13 July 2022
Published Online: 31 July 2022

Keywords:
Termite-resistance
Raw and heated tung oil
Vernicia fordii
Coptotermes formosanus

ABSTRACT

In worldwide, the use of chemical pesticides to protect wood has been greatly restricted. In recent years, a large number of researchers devoted to the search for natural, safe and non-polluting bioactive chemical compounds from plants as an alternative to synthetic organic chemical preservative. In Chinese folk, tung oil can be used as paint for wooden furniture to protect them from pests. This study aimed to evaluate the chemical compositions of raw and heated tung oil and their activity against termite. In choice bioassays, weight loss of wood treated with 5% raw or heated tung oil after 4 weeks was significantly less than that of the control group. In no-choice bioassays, there was a significant difference in termite survival and wood weight loss on raw and heated tung oil-treated wood. When tung oil-treatment concentrations increased to 5%, wood weight loss was less than 10%. There was no significant difference in termite survival and wood weight loss between raw and heated tung oil-treated wood. Survival of termites in both tung oil wood treatments was significantly lower than that in the starvation control after 4 weeks. Raw and heated tung oil significantly improved the resistance of pine wood to termites, and have the potential for the development of natural wood preservatives.

1. Introduction

Coptotermes formosanus (Shiraki) is an economically important insect pest that damages wooden structures [1]. Rust and Su [2] reported that the worldwide economic loss caused by this species is at least $40 billion annually. Ammonium copper quaternary (ACQ), copper citrate (CC), and copper chrome arsenic (CCA) have been used to treat wood and prevent termite damage, but these compounds can affect human health and the environment [3]. Therefore, there is interest in more environment-friendly, convenient, and effective wood preservatives. Some wood

*Corresponding Author:
Yongjian Xie,
College of Advanced Agricultural Sciences, Zhejiang A&F University, Hangzhou 311300, China;
Email: yjxie@zafu.edu.cn

DOI: https://doi.org/10.30564/jbr.v4i3.4793

is naturally resistant to termites [1,4], due to their active compounds that act as toxicants [2,5]. These plant compounds include tannins [4], flavonoids [6,7], alkaloids [8,9], quinones [10-12], terpinoids [13-15], and resins [16-18]. Many studies have documented that active compounds possess antitermitic properties [13,14,19].

Tung tree, *Vernicia fordii* (Hemsl), native to China, is widely cultivated in China and other countries for its industrial values [20,21]. *V. fordii* is mainly distributed in Sichuan, Hubei, Guizhou, and Hunan provinces and Chongqing municipality, which is the main production base of tung oil in China [22,23]. Tung oil, extracted from seeds, shows rapid drying, insulation, anticorrosion, acid, and alkali resistance [24]. These properties make tung oil a valuable additive in paints, varnishes, and other coatings and finishes [25]. In addition, tung tree seeds, roots, flowers, and leaves are widely used in folk medicine. Tung oil can treat burns, scalds, and cold injuries [26]. Termites are important pests of wooden structures. Many essential oils have antitermitic activities, including oils from *Lippia spp*. [27], *Artemisia absinthium* [28], *Lippia sidoides* [29], *Chamaecyparis formosensis* [30], *Liquidambar orientalis*, and *Valeriana wallichii* [31]. Hutchins [32] reported that *Aleurites fordii* wood and meal extracts had antitermitic toxicity. Tung seed is considered a good wood preservative in Chinese and is used to treat indoor and outdoor wooden furniture to protect them against insect pests and wood-rot fungi. However, the protection against termite damage offered by tung oil treatment of wood is unclear. Therefore, the purpose of this study was to compare the chemical composition of raw and heated tung oil and to determine the toxicity of raw and heated tung oil to termites.

2. Materials and Methods

2.1 Chemicals

The fatty acid methyl ester standard was obtained from Dr. Ehrenstorfer GmbH. Methanol and isooctane were purchased from Sigma Aldrich Inc, St. Louis, MO, USA. Potassium hydroxide and sodium bisulfate were obtained from Sinopharm Chemical Reagent Co., Ltd (Beijing, China).

2.2 Tung Oil

Tung oil can be divided into raw tung oil and heated tung oil. Raw tung oil was obtained from tung seeds using a hydraulic press at room temperature, with characters of golden yellow and strong penetration. Heated tung oil was made by heating the raw tung oil to 180 °C, brown color, low transparency, and high density. The oils were supplied by the Yiyousheng home exclusive store, Tmall.com. The colors of the raw and heated tung oil were light yellow brown and dark brown, respectively.

2.3 Esterification of Tung Oil Fatty Acids

The esterification of tung oil fatty acid was pretreated according to ISO 5509-2000. A 0.010 g oil sample and 1 mL of 1 M KOH-methanol solution were added to a round bottom flask and heated in a water bath at 75 °C for 10 min. After cooling to room temperature, 1 mL of C15:0 was added to the mixture. After transfer to a 250 mL separating funnel, 20 mL of n-heptane and 20 mL of water were added to stratify the mixture, and then we collected the ester layer and dried it with anhydrous sodium sulfate.

2.4 Gas Chromatography-mass Spectrometry (GC-MS)

GC-MS analysis was performed on a gas chromatograph Agilent 6890A interfaced with an Agilent 5975C mass spectrometer (Agilent Technologies (China) Co., Ltd.). An HP-5 MS capillary column (30 m × 0.25 mm × 0.25 μm) was used. The column temperature was programmed to rise from 50 °C to 280 °C at a rate of 10 °C/min. The carrier gas was helium with a flow rate of 1 mL/min. MS readings were taken at 70 eV and a mass range of 15-500. Identification of compounds of the tung oil was based on standard samples, and NIST11.LIB (National Institute of Standards and Technology) was used for qualitative analysis.

2.5 Oil Treatment

The vacuum-soak impregnation method by Nakayama and Osbrink [33] was used with slight modifications. Masson pine (*Pinus massoniana*) was cut into wood pieces that were 23 mm (length) × 14 mm (width) × 9 mm (thickness). These were sterilized in an oven at 130 °C for 24 h and weighed, and the weights were recorded. The wood was placed into a closed pressure chamber with vacuum level of –0.098 MPa for 30 min. Then, the wood specimens were immersed with different concentrations of both raw and heated tung oil-acetone mixtures, soaked for 30 min, and removed. Excess liquid on the wood surface was dried with paper, and the blocks were dried in a vacuum oven at 60 °C for 24 h. This procedure was used to remove the acetone fraction. The oil content of the oil-treated wood (%, w/w) was determined based on the gain in weight of the untreated wood.

2.6 Termites

The colonies of *Coptotermes formosanus* Shiraki were collected from Tiantong Mountain in Ningbo, Zhejiang province. The termites were reared on masson pine blocks (200 mm ×35 mm×20 mm), water soaked in plastic containers (460 mm × 36 mm × 28 mm) at 26 ± 1 °C and 80 ± 5% RH. Termites were identified using keys for soldier identification from Scheffrahn and Su [34].

2.7 Termite Resistance Test

The choice and no-choice bioassay methods of Nakayama and Osbrink [33] were used to evaluate termite resistance of pine wood treated with tung oil.

2.7.1 Choice Bioassays

The wood specimens tested contained raw and processed tung oil contents of 1.25%, 2.5%, 5.0%, 10.0%, 20.0%, and 40.0% (w/w). The termite control group was exposed to pine treated only with acetone. Two blocks of wood were placed on a sand surface on both sides of the bottom of the container (65 mm (diameter) × 90 mm (high)) (Figure 1). A total of 150 workers and 5 soldiers were placed in the container. Three replicates of the oil treatments were performed. All the testing containers were placed in a conditioning room at 26 ± 1 °C, and after 4 weeks, the wood specimens were dried and reweighed to determine wood weight loss. ASTM [35] ratings were determined for each wood block over the same period. The ASTM rating had a scale of 10-0 with 10 being sound wood with only surface nibbles permitted, 9 light attack, 7 moderate attack with penetration, 4 heavy attack, and 0 failure.

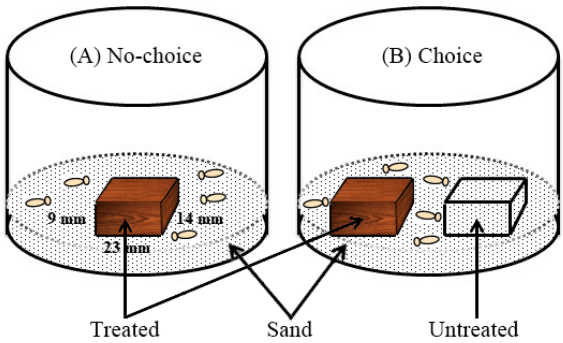

Figure 1. A test unit for evaluating termite resistance to wood treated in the laboratory. A: No-choice; B: Choice

2.7.2 No-choice Bioassays

The experimental method was the same as above, but only one piece of treated wood was placed in the middle of the container.

2.8 Statistical Analysis

For choice bioassays, Student's t test was used to compare wood specimen weight loss of untreated with treated wood specimens after 4 weeks. Differences in survival, wood specimen weight loss, and percent weight loss of wood were compared using ANOVA followed by the Student-Newman-Keuls test ($p < 0.05$).

3. Results

3.1 Chemical Compositions of Tung Oil

GC-MS analysis results of the raw and heated tung oil are shown in Table 1. The main components of raw tung oil were α-eleostearic acid (69.02%), oleic acid (12.28%), and linoleic acid (8.93%). α-eleostearic acid (65.31%), oleic acid (15.52%), and linoleic acid (9.44%) were the major components of the heated tung oil.

Table 1. Chemical composition (%) of raw and heated tung oil

No.	RI[a]	Compounds	Raw	Heated
1	1973	Palmitic acid	3.24	4.16
2	2123	Linoleic acid	8.93	9.44
3	2134	Oleic acid	12.28	15.52
4	2179	Stearic Acid	2.58	3.27
5	2482	α-eleostearic acid	69.02	65.31

[a]RI, retention index calculated on the HP-5MS column relative to C_8-C_{28} n-alkanes.

3.2 Choice Bioassays

There was significantly less wood weight loss of the blocks with 5% raw and heated tung oil after 4 weeks (Table 2) than in the untreated blocks. There was high termite survival in both tung oil treatments at 4 weeks. There were significant differences in termite survival and wood weight loss ($F = 5.406$, $df = 6, 14$, $P < 0.004$; $F = 16.374$, $df = 6, 14$, $P < 0.0001$) on raw and heated tung oil-treated wood, respectively. These results were corroborated using the ASTM rating system (Table 3).

Table 2. Comparison of weight loss between wood specimens treated with both raw and heated tung oil 4 weeks after exposure to *C. formosanus* in the feeding choice bioassays.

Treatment % (w/w)	Survival, %	Weight loss (mg) and t statistics (mean ± SD)			
		Treated	Untreated	t	*P*
raw tung oil					
40	78.0 ± 3.1d	36.7 ± 29.1	271.8 ± 37.2	8.63	0.001
20	89.8 ± 5.7ab	61.3 ± 27.8	249.4 ± 38.3	6.89	0.002
10	81.6 ± 3.0cd	85.1 ± 34.0	247.3 ± 19.7	7.16	0.002
5	81.1 ± 3.8cd	102.0 ± 60.9	243.1 ± 23.1	3.75	0.02
2.5	82.2 ± 2.7cd	191.5 ± 50.7	221.1 ± 58.9	0.66	0.55
1.25	90.4 ± 2.3ab	278.2 ± 62.2	236.3 ± 18.6	1.12	0.33
heated tung oil					
40	80.2 ± 1.1cd	33.8 ± 11.2	298.5 ± 23.9	17.34	0.0001
20	87.8 ± 2.0abc	50.1 ± 12.1	321.0 ± 67.7	6.83	0.002
10	82.0 ± 2.4cd	55.8 ± 21.5	279.2 ± 64.3	5.70	0.005
5	93.8 ± 1.7a	73.8 ± 18.0	271.7 ± 54.8	5.94	0.004
2.5	81.3 ± 2.4cd	206.2 ± 55.1	242.2 ± 40.3	0.91	0.41
1.25	90.7 ± 2.9ab	237.7 ± 28.7	257.5 ± 52.0	0.58	0.60
Control					
Acetone	85.3 ± 3.1bcd	259.4 ± 32.1	253.0 ± 35.8	0.23	0.83
Untreated	84.7 ± 2.4bcd	212.5 ± 26.9	242.5 ± 107.9	0.47	0.67

Table 3. Comparison of ASTM ratings between wood specimens treated with both raw and heated tung oil and untreated wood specimens 4 weeks after exposure to *C. formosanus* in a feeding choice bioassay.

Treatment % (w/w)	ASTM rating of wood and t statistics (mean ± SD)[a]			
	Treated	Untreated	t	*P*
raw tung oil				
40	9.7 ± 0.6	0.0 ± 0.0	29.00	0.001
20	9.3 ± 0.6	0.0 ± 0.0	28.00	0.001
10	8.8 ± 0.3	0.0 ± 0.0	53.00	0.0001
5	7.7 ± 1.2	0.0 ± 0.0	11.5	0.007
2.5	4.7 ± 1.2	3.7 ± 1.5	0.655	0.58
1.25	4.0 ± 1.0	3.3 ± 0.6	1.09	0.423
heated tung oil				
40	9.8 ± 0.3	0.0 ± 0.0	59.00	0.0001
20	9.5 ± 0.5	0.0 ± 0.0	32.91	0.001
10	9.3 ± 0.0	0.0 ± 0.0	28.00	0.001
5	8.7 ± 1.5	0.0 ± 0.0	9.827	0.01
2.5	4.0 ± 1.0	3.7 ± 1.2	1.09	0.423
1.25	5.0 ± 1.7	4.0 ± 1.5	2.01	0.184
Control				
Acetone	4.3 ± 0.6	5.0 ± 1.7	0.555	0.635
Untreated	4.3 ± 1.5	4.6 ± 2.1	0.229	0.84

[a] ASTM scale of 10-0 with 10 being sound, surface nibbles permitted, 9 having light attack, 7 moderate attack with penetration, 4 with heavy attack, and 0 failure.

3.3 No-choice Bioassays

There were significant differences in termite survival ($F = 72.87$; $df = 6, 14$, $P < 0.0001$; $F = 39.83$, $df = 1, 97$, $P < 0.0001$) and wood weight loss ($F = 44.32$, $df = 4, 16$, $P < 0.0001$; $df = 4, 16$, $F = 50.97$, $P < 0.0001$) on raw and heated tung oil-treated wood, respectively. Survival and wood weight loss in both tung oil-treatments decreased as the concentration increased (Table 4). When the raw and treated tung oil concentrations increased to 5.0%, percent weight loss of wood was less than 10% (Table 4). ASTM ratings were highest when both raw and heated tung oil content was 40% (Table 5). There were no significant differences in termite survival ($F = 0.257$; $df = 5, 36$; $P = 0.932$) and wood specimen weight loss ($F = 0.403$; $df = 5, 36$; $P = 0.842$) on raw and heated tung oil-treated wood.

Table 4. Comparison of termite survival and wood specimens weight loss between wood specimens treated with both raw and heated tung oil 4 weeks after exposure to *C. formosanus* in the feeding no-choice bioassays.

Treatment % (w/w)	mean ± SD[a]		
	Survival, %	Total wt loss, mg	Percent weight loss, %
raw tung oil			
40	26.7 ± 2.4e	36.5 ± 4.5d	1.9 ± 0.2d
20	45.1 ± 2.1d	96.5 ± 20.5bc	5.4 ± 1.1cd
10	47.3 ± 1.3cd	138.8 ± 15.0b	6.9 ± 0.8cd
5	48.7 ± 6.6cd	168.4 ± 28.4b	10.2 ± 1.7c
2.5	55.3 ± 2.7bcd	256.1 ± 29.6a	17.3 ± 2.0b
1.25	63.1 ± 5.2b	281.7 ± 22.8a	17.0 ± 1.4b
heated tung oil			
40	27.8 ± 2.0e	54.3 ± 23.8cd	2.6 ± 1.2d
20	49.1 ± 5.6cd	105.8 ± 12.4bc	6.1 ± 0.7cd
10	51.8 ± 6.0cd	141.4 ± 6.1b	8.4 ± 0.4c
5	55.3 ± 2.7bcd	163.4 ± 9.6b	8.9 ± 0.5c
2.5	58.4± 2.8bc	280.9 ± 21.2a	18.2 ± 1.4b
1.25	65.8 ± 8.4b	294.7 ± 30.0a	23.5 ± 2.4a
Control			
Acetone	84.7 ± 4.8a	284.4 ± 67.0a	24.5 ± 5.7a
Untreated	86.2 ± 2.8a	312.2 ± 45.7a	24.6 ± 3.6a
No food	83.1 ± 5.4a	-	-

[a] Means ± SD followed by the different letter within a column are significantly different ($P < 0.05$; using Student-Newman-Keuls test).

Table 5. Comparison of ASTM ratings between wood specimens treated with both raw and heated tung oil and untreated wood specimens 4 weeks after exposure to *C. formosanus* in a feeding no-choice bioassay.

Treatment % (w/w)	ASTM rating of wood (mean ± SD)[a]	
	raw tung oil	heated tung oil
40	9.7 ± 0.6a	9.3 ± 0.6A
20	8.3 ± 1.5ab	8.0 ± 1.0B
10	6.7 ± 2.5b	6.3 ± 0.6C
5	4.6 ± 0.6c	4.3 ± 1.5D
2.5	0.0 ± 0.0d	0.0 ± 0.0E
1.25	0.0 ± 0.0d	0.0 ± 0.0E
Acetone	0.0 ± 0.0d	0.0 ± 0.0E
Untreated	0.0 ± 0.0d	0.0 ± 0.0E

[a] ASTM scale of 10-0 with 10 being sound, surface nibbles permitted, 9 having light attack, 7 moderate attack with penetration, 4 with heavy attack, and 0 failure.

4. Discussion

Biodegradation of wood by fungi and termites is a serious problem for wooden structures world-wide [15]. The alkaline copper quat (ACQ) [36], boron-fluorine-chromium-arsenic (BFCA salts) [37], copper azole (CA) [38], copper chrome arsenate (CCA) [39], chlorotalonil (CTL) [36], copper- and zinc-salicylate [40], quaternary ammonium compounds (QACs) [41], siloxane [42], sodium fluoride (NaF) [43-45], and zinc borate [46] have been used to protect wood against termite damage. Besides these, nanoparticles from zinc oxide (ZnO) [47,48], CuO and B_2O_3 [49], and magnesium fluoride (MgF_2) [50] have provided promising levels of protection. Wood preservatives should ideally be environmentally friendly; thus, there is interest in safer alternative wood protection methods. Secondary plant compounds in some species of wood play a major role in the protection of wood against termite attack [51-55]. Here, we evaluated the chemical composition of tung oil and tested their activity against termite.

The major components of tung oil studied in this paper are similar to previous reports on this species. Raw tung oil, extracted from seeds, contains 60%~80% α-eleostearic acid and is used for the production of biodiesel, dyes, inks, and resins [20,56,57]. The α-eleostearic acid has a po-

tential role in human health products such as those with antibacterial [58], antitumor [59], anti-neuroinflammatory [26], antioxidative [60], and antiobesity [61] activity. It also provides a reference on the safety of tung oil used in commercial applications. In addition, α-eleostearic acid can prevent *Anthonomus grandis* damage to cotton bolls [62]. Thus, high anti-termitic properties of tung oil could be due to the high toxicity of its major component α-eleostearic acid. Similarly, Xie et al. [15] showed that the major constituents of *Syzgium aromaticum*, eugenol, against *Reticulitermes chinensis* for 1 d, 3 d and 5 d had LC_{50} values of 38.0 μg/g, 12.1 μg/g, and 9.2 μg/g, respectively. Yang et al. [63] also demonstrated that the high toxicity of *Mentha spicata* EO against *Reticulitermes dabieshanensis* was attributed to its major components, carvone, limonene and dihydrocarvone.

In choice experiments, there was no significant difference in termite survival and wood weight loss between raw and heated tung oil-treated wood. Therefore, raw tung oil can be directly used for wood preservation to reduce the processing cost of heated tung oil. Under starvation conditions for 4 weeks, termite survival was significantly higher than that of raw and heated tung oil-treated wood, indicating that raw and heated tung oil were feeding deterrents for *C. formosanus*. Similar results were obtained showing that tung wood and meal have antitermitic properties [32]. In addition, Nakayama and Osbrink [33] showed that *A. moluccana* oil-treated wood was resistant to *C. formosanus*. Taylor et al. [64] observed that removal of the methanol-soluble heartwood components of *Thuja plicata* and *Chamaecyparis nootkatensis* reduced their resistance to termite attack. Syofund et al. [65] observed that wood extracts used as preservatives improved the resistance of less durable wood to termite attack by 50% compared to the controls. Brocco et al. [66] found that ethanol extracts of *Tectona grandis* heartwood increased the resistance and mortality against *Nasutitermes corniger* in both choice and no-choice tests. Similar results were reported by Hassan et al. [67], who showed that *Tectona grandis* and *Cedrus deodara* extracts imparted termite resistance to non-durable wood species.

5. Conclusions

In this study, we investigated the resistance of pine wood (*P. massoniana*), treated with raw and heated tung oil, to the termite, *C. formosanus*. Our study demonstrated that both tung oil treatments significantly improved the resistance of pine wood to termites. When both tung oil-treated concentrations were 5.0%, the weight loss of wood was less than 10%. There was no significant difference in termite survival rate and wood weight loss between the two tung oil treatments. Therefore, raw tung oil can be directly used for wood preservation to reduce the processing cost of heated tung oil. In addition, the use of tung oil for wood preservative treatment can expand the demand for tung oil and increase local economic income.

Acknowledgments

This study was funded by College Students' Scientific Research Training Program of Zhejiang A&F University (No. 113-2013200148) and ZAFU-Institute of Termite Control of Yuhang cooperative project (2045200485, 2045200529).

Conflict of Interest

There is no conflict of interest.

References

[1] Cornelius, M.L., Osbrink, W.L.A., 2015. Natural resistance of exotic wood species to the Formosan subterranean termite (Isoptera: Rhinotermitidae). International Biodeterioration & Biodegradation. 101, 8-11.
DOI: http://dx.doi.org/10.1016/j.ibiod.2015.03.016

[2] Rust, M.K., Su, N.Y., 2012. Managing social insects of urban importance. Annual Review of Entomology. 57, 355-375.
DOI: https://doi.org/10.1146/annurev-ento-120710-100634

[3] Chen, P.S., Chen, Y.H., Yeh, T.F., et al., 2014. Mechanism of decay resistance of heartwood extracts from *Acacia confusa* against the brown-rot fungus *Laetiporus sulphureus*. Wood Science and Technology. 48, 451-465.
DOI: https://doi.org/10.1007/s00226-014-0615-6

[4] Santana, A.L.B.D., Maranhão, C.A., Santos, J.C., et al., 2010. Antitermitic activity of extractives from three Brazilian hardwoods against *Nasutitermes corniger*. International Biodeterioration & Biodegradation. 64, 7-12.
DOI: https://doi.org/10.1016/j.ibiod.2009.07.009

[5] Roszaini, K., Nor Azah, M.A., Mailina, J., et al., 2013. Toxicity and antitermite activity of the essential oils from *Cinnamomum camphora*, *Cymbopogon nardus*, *Melaleuca cajuputi* and *Dipterocarpus sp*. against *Coptotermes curvignathus*. Wood Science and Technology. 47, 1273-1284.
DOI: https://doi.org/10.1007/s00226-013-0576-1

[6] Reyes-Chilpa, R., Viveros-Rodríguez, N., Gomez-Garibay, F., et al., 1995. Antitermitic activity of *Lonchocarpus castilloi* flavonoids and heartwood

extracts. Journal of Chemical Ecology. 21, 455-463.
DOI: https://doi.org/10.1007/BF02036742

[7] Ohmura, W., Doi, S., Aoyama, M., 2000. Antifeedant activity of flavonoids and related compounds against the subterranean termite *Coptotermes formosanus* Shiraki. Journal of Wood Science. 46, 149-153.
DOI: http://doi.org/10.1007/BF00777362

[8] Kawaguchi, H., Kim, M., Ishida, M., et al., 1989. Several antifeedants from *Phellodendron amurense* against *Reticulitermes speratus*. Agricultural and Biological Chemistry. 53, 2635-2640.
DOI: https://doi.org/10.1080/00021369.1989.10869702

[9] Mao, L., Henderson, G., 2007. Antifeedant activity and acute and residual toxicity of alkaloids from *Sophora flavescens* (Leguminosae) against Formosan subterranean termites (Isoptera: Rhinotermitidae). Journal of Economic Entomology. 100, 866-870.
DOI: https://doi.org/10.1039/b406975g

[10] Ganapaty, S., Thomas, P.S., Fotso, S., et al., 2004. Antitermitic quinones from *Diospyros sylvatica*. Phytochemistry. 65, 1265-1271.
DOI: http://doi.org/10.1016/j.phytochem.2004.03.011

[11] Lukmandaru, G., Takahashi, K., 2008. Variation in the natural termite resistance of teak (*Tectona grandis* Linn fil.) wood as a function of tree age. Annals of Forest Science. 65, 708.
DOI: https://doi.org/10.1112/S0024610700001022

[12] Lukmandaru, G., Takahashi, K., 2009. Radial distribution of quinones in plantation teak (*Tectona grandis* L.f.). Annals of Forest Science. 66, 605.
DOI: https://doi.org/10.1051/forest/2009051

[13] Watanabe, Y., Mihara, R., Mitsunaga, T., et al., 2005. Termite repellent sesquiterpenoids from *Callitris glaucophylla* heartwood. Journal of Wood Science. 51, 514-519.
DOI: https://doi.org/10.1007/s10086-004-0683-6

[14] Xie, Y.J., Wang, K., Huang, Q.Y., et al., 2014. Evaluation toxicity of monoterpenes to subterranean termite, *Reticulitermes chinensis* Snyder. Industrial Crops and Products. 53, 163-166.
DOI: https://doi.org/10.1016/j.indcrop.2013.12.021

[15] Xie, Y.J., Yang, Z.L., Cao, D.Y., et al., 2015. Antitermitic and antifungal activities of eugenol and its congeners from the flower buds of *Syzgium aromaticum* (Clove). Industrial Crops and Products. 77, 780-786.
DOI: https://doi.org/10.1016/j.indcrop.2015.09.044

[16] Bultman, J.D., Gilbertson, R.K., Adaskaveg, J., 1991. The efficacy of guayule resin as a pesticide. Bioresource Technology. 35, 1997-2001.
DOI: https://doi.org/10.1016/0960-8524(91)90030-N

[17] Bultman, J.D., Chen, S.L., Schloman, W.W.Jr., 1998. Antitermitic efficacy of the resin and rubber in fractionator overheads from a guayule extraction process. Industrial Crops and Products. 8, 133-143.
DOI: https://doi.org/10.1016/S0926-6690(97)10018-8

[18] Nakayama, F.S., Vinyard, S.H., Chow, P., et al., 2001. Guayule as a wood preservative. Industrial Crops and Products. 14, 105-111.
DOI: https://doi.org/10.1016/S0926-6690(00)00093-5

[19] Hu, J.B., Chang, S.S., Peng, K.Y., et al., 2015. Bio-susceptibility of shells of *Camellia oleifera* Abel fruits to fungi and termites. International Biodeterioration & Biodegradation. 104, 219-223.
DOI: https://doi.org/10.1016/j.ibiod.2015.06.011

[20] Cui, P., Lin, Q., Fang, D., et al., 2018. Tung tree (*Vernicia fordii*, Hemsl) genome and transcriptome sequencing reveals co-ordinate up-regulation of fatty acid beta-oxidation and triacylglycerol biosynthesis pathways during eleostearic acid accumulation in seeds. Plant and Cell Physiology. 59, 1990-2003.
DOI: http://doi.org/10.1093/pcp/pcy117

[21] Liu, M., Li, W., Zhao, G., et al., 2019. New insights of salicylic acid into stamen abortion of female flowers in tung tree (*Vernicia fordii*). Frontiers in Genetics. 10, 316.
DOI: https://doi.org/10.3389/fgene.2019.00316

[22] Zhang, L.L., Luo, M.C., You, F.M., et al., 2015. Development of microsatellite markers in tung tree (*Vernicia fordii*) using cassava genomic sequences. Plant Molecular Biology Reporter. 33, 893-904.
DOI: http://doi.org/10.1007/s11105-014-0804-3

[23] Zhang, L.L., Lu, S.Y., Sun, D.F., et al., 2015. Genetic variation and geographic differentiation revealed using ISSR markers in tung tree, *Vernicia fordii*. Journal of Genetics. 94, e5-9.
DOI: http://doi.org/10.1007/s12041-015-0473-5

[24] Chen, J., Liu, W., Fan, Y., et al., 2019. Identification and analysis of tRNA genes provide new insights into oil biosynthesis in tung tree (*Vernicia fordii* Hemsl). Industrial Crops and Products. 137, 74-80.
DOI: https://doi.org/10.1016/j.indcrop.2019.05.016

[25] Li, Z., Shi, K., Zhang, F., et al., 2019. Growth, physiological, and biochemical responses of tung tree (*Vernicia fordii*) seedlings to different light intensities. Hortscience. 54, 1361-1369.
DOI: https://doi.org/10.21273/HORTSCI14035-19

[26] Chen, G., Zhao, W., Li, Y., et al., 2020. Bioactive chemical constituents from the seed testa of *Vernicia fordii* as potential neuroinflammatory inhibitors. Phytochemistry. 171, 112233.
DOI: https://doi.org/10.1016/j.phytochem.2019.112233

[27] Santos, D.R., Oliveira, L.M., Lucchese, A.M., et al.,

2020. Insecticidal activity of essential oils of species from the genus *Lippia* against *Nasutitermes corniger* (Motschulsky) (Isoptera: Termitidae). Sociobiology. 67, 292-300.
DOI: https://doi.org/10.13102/sociobiology.v67i2.4992

[28] Mishra, T., Gangoo, S.A., Azad, A., et al., 2020. Chemical composition and antitermite activity of essential oil from *Artemisia absinthium* growing in Kashmir Valley of India. Journal of Essential Oil Bearing Plants. 23, 397-404.
DOI: https://doi.org/10.1080/0972060X.2020.1731335

[29] Santos, A.A., de Oliveira, B.M.S., Melo, C.R., et al., 2017. Sub-lethal effects of essential oil of *Lippia sidoides* on drywood termite *Cryptotermes brevis* (Blattodea: Termitoidea). Ecotoxicology and Environmental Safety. 145, 436-441.
DOI: https://doi.org/10.1016/j.ecoenv.2017.07.057

[30] Hsu, C.Y., Lin, C.Y., Chang, S.T., 2016. Antitermitic activities of wood essential oil and its constituents from *Chamaecyparis formosensis*. Wood Science and Technology. 50, 663-676.
DOI: https://doi.org/10.1007/s00226-016-0811-7

[31] Park, I.K., 2014. Fumigant toxicity of Oriental Sweetgum (*Liquidambar orientalis*) and Valerian (*Valeriana wallichii*) Essential oils and their components, including their Acetylcholinesterase inhibitory activity, against Japanese Termites (*Reticulitermes speratus*). Molecules. 19, 12547-12558.
DOI: https://doi.org/10.3390/molecules190812547

[32] Hutchins, R.A., 2001. Tung tree extracts useful for controlling termites. U.S. Patent No. 6, 264, 956.

[33] Nakayama, F.S., Osbrink, W.L., 2010. Evaluation of kukui oil (*Aleurites moluccana*) for controlling termites. Industrial Crops and Products. 31, 312-315.
DOI: http://doi.org/10.1016/j.indcrop.2009.11.009

[34] Scheffrahn, R.H., Su, N.Y., 1994. Keys to soldiers and winged adult termites (Isoptera) of Florida. Florida Entomologist. 77, 460-474.
DOI: http://doi.org/doi:10.2307/3495700

[35] American Society for Testing and Materials (ASTM), 1998. Standard test method for laboratory evaluation of wood and other cellulosic materials for resistance to termites, Standard D 3345-74. Annual Book of ASTM Standards 4.10. ASTM, West Conshohocken, PA. pp. 430-432.

[36] Tascioglu, C., Tsunoda, K., 2010. Laboratory evaluation of wood-based composites treated with alkaline copper quat against fungal and termite attacks evaluated. International Biodeterioration & Biodegradation. 64, 683-687.
DOI: https://doi.org/10.1016/j.ibiod.2010.05.010

[37] Bayatkashkoli, A., Kameshki, B., Ravan, S., et al., 2017. Comparing of performance of treated particleboard with alkaline copper quat, boron-fluorine-chromium-arsenic and chlorotalonil against *Microcerotermes diversus* and *Anacanthotermes vagans* termite. International Biodeterioration & Biodegradation. 120, 186-191.
DOI: http://dx.doi.org/10.1016/j.ibiod.2017.03.003

[38] Lin, L.D., Chen, Y.F., Wang, S.Y., et al., 2009. Leachability, metal corrosion and termite resistance of wood treated with copper-based preservative. International Biodeterioration & Biodegradation. 63, 533-538.
DOI: https://doi.org/10.1016/j.ibiod.2008.07.012

[39] Mugabi, P., Otuko, E., 2019. Effectiveness of copper chrome arsenate and used engine oil in protecting fencing post of ugandan grown eucalypt clone GC550 and *Phoenix reclinata* against termite attack. Maderas-Ciencia y Tecnologia. 21, 97-104.
DOI: http://dx.doi.org/10.4067/S0718-221X2019005000109

[40] Bayatkashkoli, A., Taghiyari, H.R., Kameshki, B., et al., 2016. Effects of zinc and copper salicylate on biological resistance of particleboard against *Anacanthotermes vagans* termite. International Biodeterioration & Biodegradation. 115, 26-30.
DOI: https://doi.org/10.1016/j.ibiod.2016.07.013

[41] Terzi, E., Tasçioglu, C., Kartal, S.N., et al., 2011. Termite resistance of solid wood and plywood treated with quaternary ammonia compounds and common fire retardants. International Biodeterioration & Biodegradation. 65, 565-568.
DOI: https://doi.org/10.1016/j.ibiod.2010.10.014

[42] Gascón-Garrido, P., Thévenon, M.F., Mainusch, N., et al., 2017. Siloxane-treated and copper-plasma-coated wood: Resistance to the blue stain fungus *Aureobasidium pullulans* and the termite *Reticulitermes flavipes*. International Biodeterioration & Biodegradation. 120, 84-90.
DOI: http://dx.doi.org/10.1016/j.ibiod.2017.01.033

[43] Pan, C., Wang, C., 2015. Sodium fluoride for protection of wood against field populations of Subterranean Termites. Journal of Economic Entomology. 108, 2121-2124.
DOI: https://doi.org/10.1093/jee/tov175

[44] Pan, C., Ruan, G., Chen, H., et al., 2015. Toxicity of sodium fluoride to subterranean termites and leachability as a wood preservative. European Journal of Wood and Wood Products.73, 97-102.

DOI: https://doi.org/10.1007/s00107-014-0849-x

[45] Tascioglu, C., Umemura, K., Kusuma, S.S., et al., 2017. Potential utilization of sodium fluoride (NaF) as a biocide in particleboard production. Journal of Wood Science. 63, 652-657.
DOI: https://doi.org/10.1007/s10086-017-1654-z

[46] Xuan, L., Hui, D., Cheng, W., et al., 2017. Effect of Preservative Pretreatment on the Biological Durability of Corn Straw Fiber/HDPE Composites. Materials. 10, 789.
DOI: http://dx.doi.org/10.3390/ma10070789

[47] Akhtari, M., Nicholas, D., 2013. Evaluation of particulate zinc and copper as wood preservatives for termite control. European Journal of Wood and Wood Products. 71, 395-396.
DOI: http://dx.doi.org/10.1007/s00107-013-0690-7

[48] Mantanis, G., Terzi, E., Kartal, S.N., et al., 2014. Evaluation of mold, decay and termite resistance of pine wood treated with zinc- and copper-based nanocompounds. International Biodeterioration & Biodegradation. 90, 140-144.
DOI: http://dx.doi.org/10.1016/j.ibiod.2014.02.010

[49] Terzi, E., Kartal, S.N., Yılgor, N., et al., 2016. Role of various nano-particles in prevention of fungal decay, mold growth and termite attack in wood, and their effect on weathering properties and water repellency. International Biodeterioration & Biodegradation. 107, 77-87.
DOI: http://dx.doi.org/10.1016/j.ibiod.2015.11.010

[50] Usmani, S.M., Plarre, R., Hübert, T., et al., 2020. Termite resistance of pine wood treated with nano metal fluorides. European Journal of Wood and Wood Products. 78, 493-499.
DOI: https://doi.org/10.1007/s00107-020-01522-z

[51] Kartal, S.N., Terzi, E., Yoshimura, T., et al., 2012. Preliminary evaluation of storax and its constituents: Fungal decay, mold and termite resistance. International Biodeterioration & Biodegradation. 70, 47-54.
DOI: https://doi.org/10.1016/j.ibiod.2012.02.002

[52] Shiny, K.S., Remadevi, O.K., 2014. Evaluation of termiticidal activity of coconut shell oil and its comparison to commercial wood preservatives. European Journal of Wood and Wood Products. 72, 139-141.
DOI: https://doi.org/10.1007/s00107-013-0755-7

[53] Kadir, R., Masseat, K., 2018. Heartwood durability of *Dyera costulata*, *Neolamarckia cadamba* and *Khaya ivorensis* trees from fast-growth plantations against subterranean termite *Coptotermes curvignathus*. Holzforschung. 72, 143-149.
DOI: https://doi.org/10.1515/hf-2017-0067

[54] Ahmed, S., Fatima, R., Hassan, B., 2020. Evaluation of different plant derived oils as wood preservative against subterranean termite *Odontotermes obesus*. Maderas-Ciencia y Tecnologia. 22, 109-120.
DOI: https://doi.org/10.4067/S0718-221X2020005000110

[55] Eller, F.J., Kirker, G.T., Mankowski, M.E., et al., 2020. Effect of burgundy solid extracted from Eastern Red Cedar heartwood on subterranean termites and Wood-decay fungi. Industrial Crops and Products. 144, 112023.
DOI: https://doi.org/10.1016/j.indcrop.2019.112023

[56] Zhan, Z., Chen, Y., Shockey, J., et al., 2016. Proteomic analysis of tung tree (*Vernicia fordii*) oil seeds during the developmental stages. Molecules. 21, 1486.
DOI: http://doi.org/10.3390/molecules21111486

[57] Zhang, L., Wu, P., Lu, W., et al., 2018. Molecular mechanism of the extended oil accumulation phase contributing to the high seed oil content for the genotype of tung tree (*Vernicia fordii*). BMC Plant Biology. 18, 248.
DOI: https://doi.org/10.1186/s12870-018-1458-3

[58] Yuan, G.F., Chen, X.E., Li, D., 2014. Conjugated linolenic acids and their bioactivities: a review. Food & Function. 5, 1360-1368.
DOI: http://doi.org/10.1039/c4fo00037d

[59] Tsuzuki, T., Tokuyama, Y., Igarashi, M., et al., 2004. Tumor growth suppression by α-eleostearic acid, a linolenic acid isomer with a conjugated triene system, via lipid peroxidation. Carcinogenesis. 25, 1417-1425.
DOI: http://doi.org/10.1093/carcin/bgh109

[60] Dhar, P., Chattopadhyay, K., Bhattacharyya, D., et al., 2006. Antioxidative effect of conjugated linolenic acid in diabetic and non-diabetic blood: an in vitro study. Journal of Oleo Science. 56, 19-24.
DOI: http://doi.org/10.5650/jos.56.19

[61] Chen, P.H., Chen, G.C., Yang, M.F., et al., 2012. Bitter melon seed oil-attenuated body fat accumulation in diet-induced obese mice is associated with cAMP-dependent protein kinase activation and cell death in white adipose tissue. Journal of Nutrition. 142, 1197-1204.
DOI: https://doi.org/10.3945/jn.112.159939

[62] Jacobson, M., Crystal, M.M., Warthen Jr, J.D., 1981. Boll weevil (*Anthonomus gradis* gradis) feeding deterrents from tung oil expressed from *Aleurites fordii*. Journal of Agricultural and Food Chemistry. 29, 591-593.
DOI: https://doi.org/10.1021/jf00105a039

[63] Yang, X., Han, H., Li, B., et al., 2021. Fumigant toxicity and physiological effects of spearmint (*Men-*

tha spicata, Lamiaceae) essential oil and its major constituents against *Reticulitermes dabieshanensis*. Industrial Crops and Products. 171, 113894.
DOI: https://doi.org/10.1016/j.indcrop.2021.113894

[64] Taylor, A.M., Gartner, B.L., Morrell, J.J., 2006. Effects of Heartwood Extractive fractions of *Thuja plicata* and *Chamaecyparis nootkatensison* wood degradation by termites or Fungi. Journal of Wood Science. 52, 147-153.
DOI: https://doi.org/10.1007/s10086-005-0743-6

[65] Syofund, A., Banana, A.Y., Nakabonge, G., 2012. Efficiency of natural wood extractives as wood preservatives against termite attack. Maderas-Ciencia y Tecnologia. 14, 155-163.
DOI: https://doi.org/10.4067/S0718-221X2012000200003

[66] Brocco, V.F., Paes, J.B., Costa, L.G., et al., 2020. Wood color changes and termiticidal properties of teak heartwood extract used as a wood preservative. Holzforschung. 74, 233-245.
DOI: https://doi.org/10.1515/hf-2019-0138

[67] Hassan, B., Mankowski, M.E., Kirker, G., et al., 2019. Ex-situ performance of extracts from naturally durable heartwood species and their potential as wood preservatives. European Journal of Wood and Wood Products. 77, 869-878.
DOI: https://doi.org/10.1007/s00107-019-01443-6

BILINGUAL PUBLISHING CO.
Pioneer of Global Academics Since 1984

Journal of Botanical Research
https://ojs.bilpublishing.com/index.php/jbr

ARTICLE

Photosynthesis of Submerged and Surface Leaves of the Dwarf Water Lily (*Nymphoides aquatica*) Using PAM Fluorometry

Tharawit Wuthirak[1] Raymond J. Ritchie[2*]

1. Department of Biology, Faculty of Science, Prince of Songkla University, Hat Yai, 90112, Thailand
2. Tropical Plant Biology Unit, Faculty of Technology and Environment, Prince of Songkla University, Phuket, 83120, Thailand

ARTICLE INFO

Article history
Received: 23 June 2022
Revised: 3 August 2022
Accepted: 5 August 2022
Published Online: 15 August 2022

Keywords:
CAM photosynthesis
SAM photosynthesis
Submerged aquatic macrophyte
Carbon fixation
Diurnal cycle
Photosynthetic oxygen evolution rate (POER)
Light curves
PAM fluorometry
Photosynthetic photon fluence rate (PPFD)
Primary productivity

ABSTRACT

Dwarf Water Lilies (*Nymphoides aquatica* (J.F. Gmel) Kuntze have floating and submerged leaves. Some submerged aquatic vascular plants have a form of CAM (Crassulacean Acid Metabolism) called Submerged Aquatic Macrophyte (SAM) metabolism. Blue-diode based PAM technology was used to measure the Photosynthetic Oxygen Evolution Rate (POER: $1O_2 \equiv 4e^-$). Optimum Irradiance (E_{opt}), maximum POER ($POER_{max}$) and quantum efficiency (α_0) all vary on a diurnal cycle. The shape of the POER *vs.* E curves is different in seedling, submerged and surface leaves. Both E_{opt} and $POER_{max}$ are very low in seedling leaves ($E_{opt} \approx 104$ µmol photon m^{-2} s^{-1}, PPFD; $POER_{max} \approx 4.95$ µmol O_2 g^{-1} Chl *a* s^{-1}), intermediate in mature submerged leaves ($E_{opt} \approx 419$ µmol photon m^{-2} s^{-1} PPFD, $POER_{max} \approx 38.1$ µmol O_2 g^{-1} Chl *a* s^{-1}) and very high in surface leaves ($E_{opt} \approx 923$ µmol photon m^{-2} s^{-1} PPFD, $POER_{max} \approx 76.1$ µmol O_2 g^{-1} Chl *a* s^{-1}). Leaf titratable acid (C4 acid pool) is too small (≈20 to 50 mol H^+ m^{-3}) to support substantial SAM metabolism. Gross daily photosynthesis of surface leaves is ≈3.71 g C m^{-2} d^{-1} in full sun and as much as 1.4 gC m^{-2} d^{-1} in shaded submerged leaves. There is midday inhibition of photosynthesis.

1. Introduction

The Dwarf Water Lily (*Nymphoides aquatica* (J.F. Gmel) Kuntze, Menyanthaceae) are ubiquitous aquatic plants, originally from SE North America but its use as an ornamental has now distributed it worldwide throughout temperate and tropical habitats. The Menyanthaceae are members of the Asterales and so the family is not part of the archaic basal group of angiosperms that includes the

*Corresponding Author:
Raymond J. Ritchie,
Tropical Plant Biology Unit, Faculty of Technology and Environment, Prince of Songkla University, Phuket, 83120, Thailand;
Email: raymond.r@phuket.psu.ac.th; Raymond.Ritchie@alumni.sydney.edu.au

DOI: https://doi.org/10.30564/jbr.v4i3.4820

Nymphaeaceae [1-3]. The Blue Water Lily (*Nymphaea caerulea* Savigny) and the Dwarf Water Lily are not closely related and might not be expected to have similar physiologies despite a shared habitat and the superficially similar appearance of the surface leaves. Unlike *Nymphaea caerulea*, *N. aquatica* has morphologically different floating leaves as well as mature functional submerged leaves. The leaves of some aquatic plants with distinctly different emergent or floating leaves compared to their fully submerged leaves are known to have different photosynthetic physiologies [4,5].

Some aquatic vascular plants such as *Isoetes* species and *Littorella uniflora* have a form of CAM (Crassulacean Acid Metabolism) known as Submerged Aquatic Macrophyte (SAM) metabolism [4,6-14]. Very little information is available on photosynthesis of water-lilies or plants with a nymphoid (water lily-like) morphology (true water lilies: Nymphaeaceae; dwarf water lilies: Menyanthaceae; Lotus lily (*Nelumbo nucifera*): Nelumboaceae) [4,14-18]). Keeley and Morton [4] found no significant nocturnal carbon fixation in *Nuphar polysepalum* (Nymphaeaceae) in their survey of SAM-physiology in aquatic plants. The blue water lily, *Nymphaea caerulea*, is also not a SAM plant [18] despite circumstantial evidence from its $^{13}C/^{12}C$ ratio [19]. Longstreth [20] reported that no example of SAM physiology had yet been found in floating or emergent leaves of aquatic plants and it does not appear that any such plants have since been identified.

Known SAM metabolism plants have a physiology closer to facultative CAM plants than obligate CAM species because they only exhibit SAM metabolism under certain conditions [21-26]. The semi-aquatic fern ally *Stylites sp.* (now part of *Isoetes*) has no functional stomata and relies on CO_2 from its roots and a SAM metabolism [8]. The fern ally, *Isoetes* species have functional stomata when growing aerially (where it behaves as a typical C3 plant) but not under water. Submergent leaves of *Isoetes* species exhibit SAM metabolism with nocturnal C4 carbon fixation and using CO_2 from its roots and not the water column [6,7,10,13]. Another fern ally, *Littorella uniflora* growing on moist mud in the air does not exhibit the SAM metabolism characteristics of submerged plants [9,13]. Thus some SAM metabolism plants obtain much of their CO_2 supply from their roots rather than from the water column or the atmosphere but there might not necessarily be a definite connection between the presence of SAM metabolism and use of CO_2 obtained by their roots. *Lobelia dortmanna* lacks stomates but nevertheless is an example of a submerged aquatic vascular plant *that does not have* SAM/CAM metabolism [27].

In the case of aquatic plants such as *N. aquatica* which has both floating and emergent leaves it would be reasonable to expect considerable physiological differences between floating and emergent leaves [28-30]. If an aquatic plant with surface leaves and submerged leaves connected by aerenchyma had SAM metabolism it would have four potential sources of inorganic carbon: (1) atmospheric CO_2 during the day, (2) atmospheric CO_2 fixed as C4 acids at night, (3) CO_2/HCO_3^- from the water column and/or (4) CO_2 arising from the roots buried in sediment and delivered to the leaves through the aerenchyma [15]. In the case of *N. aquatica* the submerged leaves could be getting their CO_2 supply from mechanisms (3) and (4) above, the later by thermosmotic air flow from the surface leaves to the roots and back to the submerged leaves [15,16,20,31-34].

Gas flow through the petioles, stems and leaves of aquatic plants, particularly species of *Nymphoides*, *Nymphaeaceae*, *Nelumbo* and mangroves has long been a source of fascination but is not well understood [34]. Pressurisation (as much as 1 kPa ~ 3 kPa) and mass flow are basically caused by thermal and humidity gradients (thermosmosis) but there are conflicting findings concerning their effects on the physiology of aquatic and amphibious plants. In *N. aquatica* and *Nymphaea caerulea* the direction of flow is from young leaves, through their petioles to the rhizome and then up the petioles of the older leaves to the mature leaves carrying some CO_2 from the mud to the mature leaves: this would account for the anomalous $^{13}C/^{12}C$ ratio found by Troxler and Richards [19].

Measurements of photosynthesis based on fluorescence methods (Pulse Amplitude Modulation-PAM fluorometry) measure the actual light reactions of photosynthesis and do not involve gas exchange measurements. PAM fluorometers can be used to monitor photosynthesis in terrestrial plants and in most photo-oxygenic algae: the key advantage of the technique is that PAM fluorometry directly measures the light reactions of PSII. PAM fluorometry is also non-destructive and large amounts of data can be collected very quickly [18,35-42]. PAM fluorometers measure the photons of light that are emitted as far-red fluorescence (>690 nm) from a flash of LED diode blue or red light or quartz halogen light and so actually measure the light reactions by subtraction (absorbed minus fluorescent photons).

Two other very important parameters calculated by PAM methods are the Electron Transport Rate (ETR) and non-photochemical quenching (NPQ). The ETR is an estimate of the number of electrons passing through Photosystem II (4 electrons pass through PSII per O_2 produced in photosynthesis from $2H_2O$) and so can be used as an estimate of the Photosynthetic Oxygen Evolution Rate (POER). This is a high estimate of gross photosynthesis

(Pg) because it does not take into account oxygen consumption by photorespiration or possible Mehler reactions [43]. PAM measurements cannot measure O_2 consumption by photorespiration, mitochondrial respiration or by Mehler reactions. Non-Photochemical Quenching is related to the magnitude of the Proton Motive Force (PMF) that exists across the thylakoids in chloroplasts and the loss of absorbed energy as waste heat [37,44-47]. The high variability of NPQ and poorly fitting kinetics makes it less useful than is sometimes supposed as a measure of photosynthetic stress [18,40,41,45,48,49].

PAM fluorometers can perform measurements of the light reactions of photosynthesis very quickly [18,35-39,42,48,50,51] and measure the light reactions directly and are not limited by O_2 and CO_2 diffusion problems [18,40,41]. The air ventilation system makes attempts to estimate photosynthesis and respiration rates in Nymphoid plants based on gas exchange using an oxygen electrode or an IRGA problematic because of difficulties in identifying the pool of gas being used as a source of CO_2. Whole-plant measurements need to be made which makes them difficult to do experimentally on anything but the smallest vascular plants. Consider the case of an IRGA probe attached to a water lily or lotus lily leaf *in situ*: the observed gas exchange would reflect CO_2 fluxes in the interconnected aerenchyma of the whole plant, not respiration and net photosynthesis of that particular leaf [15,16,20,27,28,30-34,52].

Snir et al. [14] used PAM fluorometers to measure photosynthesis of emergent leaves of *Nuphar lutea* but did not focus on the SAM metabolism issue. Ritchie [18] measured photosynthesis of the floating leaves of *Nymphaea caerulea*. It was shown that the diurnal pattern of titratable acid in the leaves of *Nymphaea caerulea* was not consistent with SAM/CAM physiology and accumulation of C4 acids was not great enough to support substantial CAM physiology [18].

The aim of the present study was to use PAM techniques to investigate photosynthesis in floating leaves and submerged leaves of *N. aquatica* and systematically determine whether either leaf type expressed significant SAM/CAM physiology. It will be shown that there is a strong diurnal effect on photosynthesis but no SAM physiology despite having fully functional surface and submerged leaves. The diurnal light curve kinetics data will be used to estimate the photosynthetic oxygen evolution rate (POER) over the course of daylight and hence model photosynthesis of a water lily bed – an important habitat for primary production in lakes, ponds and wetlands, particularly in monsoonal climates such as SE-Asia, and Northern Australia.

2. Materials and Methods

2.1 Experimental Materials

Dwarf Water Lily (*Nymphoides aquatica* (J.F. Gmel) Kuntze, Menyanthaceae) and the Blue Egyptian Water Lily (*Nymphaea caerulea*, Savigny) which was the subject of a previous photosynthesis study [18] are grown as decorative plants in circular earthenware lily pond bowls (≈30 L) on the Phuket campus of Prince Songkla University Phuket campus, Phuket Province, Thailand (Lat. 7°53'N, Long. 98°24'E) and collected for experiments in June to September 2016 within 30 m of the laboratory. The lily ponds were not fertilised, rely on rainwater most of the year and are topped up with tap water in the dry season. The water depth was only 100 mm ~ 150 mm. Phuket has a monsoon tropical climate and the experimental period was during the wet season (average precipitation: June 286 mm/month). Daylight lengths were about 12 h 15 min per day. Solar time for Phuket was -28 min 6s from Thailand Standard Time (GMT+7h) on 22 June 2016 [53]. Emergent and submergent leaves of adult plants were used. Small submergent seedlings (leaf size ≈ 5 mm ~ 20 mm) were also available but in limited amounts not large enough for assays of acid accumulation. Leaves were removed using scissors and kept floating on water in Petri dishes then blotted dry on moist filter paper immediately before PAM measurements. Leaves had to be used soon after cutting otherwise they rapidly lost turgor and photosynthesis dropped dramatically. For photosynthesis measurements during daylight plants were used within 15 to 30 min after collection and were kept in the light before measuring photosynthesis (see Appendix Table) in contrast to the protocol as used previously for Blue Water Lily, *Nymphaea caerulea* [18]. The protocol for night-time measurements followed previous practice of keeping them in the dark for about 10 min before measurement but care was taken to minimise the time between collection and measurement in the light of experience with leaves collected during daylight (see Appendix Table). The leaves were collected in a black bucket with a lid to minimise exposure to light.

2.2 PPFD Irradiance in Phuket

Information on the daily 400 nm ~ 700 nm PPFD irradiance experienced in Phuket has been published elsewhere [18,40,41]. The method for calculating irradiances is described in Ritchie [18,54] using the SMARTS software [55,56]. The calculated midday irradiance at the summer solstice (22 June) was 2115 μmol m^{-2} s^{-1} [18,40,41]. The present study was made during the wet season and so days were typical-

ly overcast with midday irradiances about 2/3 of full sunlight (≈ 1450 µmol photons m^{-2} s^{-1} PPFD but irradiance on cloudy days was as low as 500 µmol photons m^{-2} s^{-1} PPFD.

2.3 Chlorophyll Determinations

A small hole-punch (9.7 mm diameter) was used to collect 73.9 × 10^{-6} m^2 buttons of *N. aquatica* leaf tissue as described for *Nymphaea caerulea* leaves [18]. Chlorophyll was extracted in Mg carbonate-neutralized ethanol and assayed using a Shimadzu UV-1601 spectrophotometer (Shimadzu Corporation, Kyoto, Japan) and assayed using the equations of Ritchie [57]. Chl *a* was calculated as µg Chl *a* m^{-2} of projected leaf surface area and µg Chl *a* g^{-1} FW (Table 1A) and the Chl *b/a* was also calculated. Chl *b/a* ratio is more logical than the more commonly quoted Chl *a/b* ratios because Chl *a* is the primary pigment.

2.4 Pulse Amplitude Modulation Fluorometry

Light saturation curve measurements were made on the adaxial surfaces of floating *N. aquatica* leaves using a Junior PAM portable chlorophyll fluorometer (Gademann Instruments GmbH, Würzburg, Germany) fitted with a 1.5 mm diameter optic fibre and a blue diode (465±40 nm) light source. PAM parameters (Y, rETR & NPQ) were calculated using the WINCONTROL software (v2.08 & v2.13; Heinz Walz Gmbh, Effeltrich, Germany) [44,45,47] using the standard settings for rapid light curves (default absorptance factor, Abt_F = 0.84, PSI/PSII allocation factor = 0.5) (Heinz Walz Gmbh, Effeltrich, Germany) to calculate the relative Electron Transport Rate (rETR) [35,37,51]. Sets of PAM light curve measurements each took about 88 s to complete with 10 s between saturating flashes of light (0.8 s duration). The actinic light values were in order of increasing intensity and the standard Walz rapid light curve protocol was used (9 levels of light). Only one light saturation experiment was run on each leaf to avoid confounding effects of multiple experimental treatments and invalid estimates of F_o. The non-linear least squares fit routines (Microsoft-EXCEL) used in the present paper are available on Research Gate [58].

2.5 Absorptance Measurements Using the Reflectance-Absorptance-Transmittance (RAT) Monitor

Absorptances of vascular plants are often considerably different to the standard value of Abt_F = 0.84 [59,60] and so it is better to measure them experimentally. Our absorptance values for *N. aquatica* are shown in Table 1B. As found here, experimentally measured absorptance values for blue light (Abt_{465nm}) are typically found to be substantially different to the default value (in various aquatic plants [5,61], *Nymphaea caerulea* [62] and *Wolffia arrhiza* [48].

2.6 Experimental Protocol

The routine protocol used for rapid light curves in our laboratory was to measure light curves *in situ* on the intact plant (Oil Palm [42]) or to cut leaves and place them in moistened filter paper in Petri dishes in a black bag for no more than about 10 min before performing a rapid light curve (Orchids [40,63], Pineapple [41], *Nymphaea caerulea* [18] and *Davallia angustata* [49]). Longer dark preincubation protocols on cut leaves were found to be unsuitable for *N. aquatica.*

A single rapid light curve takes about 2 ½ to 3 minutes to perform and so eight replicate leaves collected at one time take about 20 minutes to process. It was noticed that E_{opt} and ETR_{max} decreased with each successive leaf in a batch if the leaves were kept in the dark. A series of experiments shown in the Appendix Table showed that cut leaves decreased rapidly in photosynthesis if kept in the dark. Both the E_{opt} and $POER_{max}$ decreased in the leaves kept in the dark and so not only did photosynthesis decrease but the *shape* of the P vs. E curves also changed. Collecting the leaves and measuring them as soon as possible after collection and keeping them in the light was found to be the most satisfactory protocol for measuring rapid light curves on *N. aquatica* in the light. Leaves collected in the night-time were cut and placed in the dark following previous standard protocols such as for *Nymphaea caerulea* [18]. Effective Yield and ETR decreased rapidly in dehydrated leaves and so flaccid leaves were rejected.

2.7 Calculation of Photosynthetic Electron Transport Rates and Other Parameters

It is found experimentally that if fluorescence yield (Y) is plotted against irradiance (E) it follows a simple exponential decay function of the form $y = e^{-kx}$ [18,39-42,48,49,63,64]. The WinControl software calculates relative ETR (rETR) based on a default leaf absorptance factor (Abt_F = 0.84). Absorptance measurements determined experimentally can then be used to recalculate actual ETR (ETR = rETR × Abt_{465nm}/Abt_F).

Since effective Y *vs*. Irradiance (E) obeys a simple exponential decay function [18,39-42,48,49,63,64], plots of ETR *vs*. E obey an exponential function of the form $y = x.e^{-x}$. This equation is known as the Waiting-in-Line model [39,65]. Equation (1) below is a form of the Waiting-in-Line equation that is easier to fit using iterative least squares methods:

$$ETR = \frac{ETR_{max} E}{E_{opt}} e^{1-E/E_{opt}} \quad (1)$$

where, following previous conventions (refs above), ETR is the Electron Transport Rate as mol e^- m^{-2} s^{-1}, ETR_{max} is a scaling constant for the maximum height of the curve, E is the Irradiance (µmol photons m^{-2} s^{-1} 400 nm ~ 700 nm PPFD) and E_{opt} is the optimum irradiance that gives maximum ETR. The maximum photosynthetic efficiency (Alpha, α_0) is the initial slope of the curve at E = 0 ($\alpha_0 = e \times ETR_{max}/E_{opt}$). Perhaps a more realistic expression is the photosynthetic efficiency at optimum irradiance ($\alpha_{Eopt} = ETR_{max}/E_{opt}$). The half-maximum photosynthesis ($ETR_{half\text{-}max}$) is reached at 0.231961 times E_{opt} and photosynthesis is also inhibited by 50% at 2.67341 times E_{opt}. Four electrons are moved through PSII for each O_2 produced in photosynthesis and so an ETR of 4 µmol e^- m^{-2} s^{-1} is *roughly* equivalent to a Photosynthetic Oxygen Evolution Rate (POER) of 1 µmol O_2 m^{-2} s^{-1}.

Non-photochemical quenching (NPQ) is reputed to be a measure of the quenching of the photochemistry of photosynthesis or the energy absorbed by the photosynthetic apparatus that is not lost as fluorescence nor is it used in photosynthetic electron transport [44,45,47]. Only NPQ and not variable fluorescence NPQ (qN) is quoted in the present study. NPQ is calculated by the WinControl software using the equations described by Genty et al. [44], van Kooten and Snel [45] and Brestic and Zivcak [47]. NPQ can be described by simple exponential saturation curves ($NPQ = NPQ_{max} \times (1\text{-}e^{-kE})$ where, NPQ_{max} is the maximum NPQ at maximum irradiance and k is an exponential constant and E is the irradiance: the ½ irradiance point giving ½ of NPQ_{max}. $NPQ_{½}$ can be used to describe the shape of the curve. $NPQ_{1/2}$ saturation values rather than k_{NPQ} are quoted in Table 2 following previous conventions [42,48,49,63]. Microsoft Excel® Software Files to fit yield, ETR, qP and NPQ *vs*. Irradiance and calculate the asymptotic errors of the fitted parameters are publically available on the internet [58].

2.8 Titratable Acid

Titratable acid was measured in a freshweight basis (FW) based on methods described previously for *Nymphaea caerulea* leaves [18], for *Davallia angustata* [49] and for the orchid *Vanda sp.* [63]. Surface and submerged leaves of adult plants were sampled on a 24 h cycle, routinely boiled and then the extracts stored frozen (–20 °C) before extraction. Sufficient supplies of the very small seedling leaves were not available for titration studies. Acid was extracted in 30 mL of distilled water by heating the leaves in a hot-water bath for 30 min. After cooling, the free acid was titrated using 5 mol m^{-3} NaOH using a standard pH meter (PH-230SD, Lutron Electronic Enterprise Co. Ltd, Taipei, Taiwan) because *N. aquatica* produced a compound which interfered with the phenolphthalein indicator used in previous studies (≈ 30 mg L^{-1}) [18,40,41,49,66]. For comparative purposes, Table 1A provides the projected leaf surface area/g FW, leaf water content (g g^{-1}FW) and the freshweight/dry weight ratio of the leaves used in the present study. Dry weights of leaves were determined on standard cut leaf disks of known surface area and freshweight dried to constant weight at 80 °C as for *Nymphaea caerulea* and *Davallia angustata* [18,49]. Titratable acid was calculated as mol H^+ g^{-1} FW: this could be converted into mol H^+ m^{-3} per unit tissue water using the data in Table 1A. Buttons of *N. aquatica* leaves cut with the cork borer were also used to calculate the relationship of fresh weight per unit projected surface area and water content per unit projected leaf surface area. These could be used to calculate mol H^+ m^{-2}.

2.9 Statistics

Significant differences were found using one-way ANOVA and the Tukey Test criterion using Microsoft Excel® for the ANOVA and to write the Tukey Test routines. Zar [67] was used as the standard statistical reference book.

3. Results

3.1 Basic Information on Leaf Material

Table 1A shows the Chlorophyll *a* (Chl *a*) and water content of *N. aquatica* leaves used in the present study. The Chl *a* content of seedling leaves and submerged leaves of adult plants were not significantly different on a projected surface area basis ($p > 0.05$) but were only about ½ that found in surface leaves. There was a small but statistically significant differences in the Chl *b/a* ratio between all the leaves (surface leaves: 0.2487±0.0029 (n=48); submerged leaves: 0.2727±0.0044 (n=10); seedling leaves: 0.2860±0.0074 (n=12)). Despite the adult plant submerged leaves being noticeably thinner than floating leaves, their water contents were not significantly different on a freshweight basis.

3.2 Titratable Acid

Round disks of leaves obtained with the cork borer had a surface area/FW ratio of $5.17(\pm0.28)\times10^{-3}$ (n = 22) m^2 g^{-1} FW for surface leaves and $7.73(\pm0.49)\times10^{-3}$ m^2 g^{-1} FW (n = 22) for submerged leaves. FW/DW ratio and water content of the material used for the acid content measurements was added to the other measurements of FW/DW ratios

Table 1. Essential information on leaves of *Nymphoides aquatica*

Table 1A Chlorophyll *a* and Water Content of *Nymphoides aquatica* leaves

	Chlorophyll *a* (mg m^{-2})	Fresh weight / Dry weight Ratio	H_2O mL/g Fresh weight
Seedling leaves	89.22±7.82 (n=12)	12.50±0.78 (n=10)	0.920±0.005 (n=10)
Submerged leaves	91.82±5.99 (n=10)	9.82±0.45 (n=39)	0.884±0.005 (n=39)
Surface leaves	190.4 ±9.9 (n=48)	8.64±0.82 (n=63)	0.888±0.005 (n=63)

Table 1B Reflectance – Absorptance–Transmittance (RAT) of *Nymphoides aquatica* leaves

	%Reflection (465 nm)	%Transmission (465 nm)	%Absorptance (465 nm)
Seedling leaves	0.49±0.52 (n=12)	8.84±1.69 (n=12)	90.7±1.9 (n=12)
Submerged leaves	2.18±1.44 (n=12)	5.88±1.77 (n=12)	91.9±2.4 (n=12)
Surface leaves	2.47±0.59 (n=20)	1.64±0.40 (n=20)	97.0±0.8 (n=20)

and leaf water contents obtained in the course of other parts of the study to give overall values (Table 1A). These data were used to convert titratable acid on a freshweight basis to titratable acid per unit projected surface area of the leaves [18].

3.3 Light Absorption Properties of Leaves

Table 1B shows the experimentally measured Reflectance, Transmission and Absorptance properties of *N. aquatica* leaves under blue light (465 nm) using the RAT monitor. Adult surface leaves of *N. aquatica* are effectively optically black in blue light: they absorb nearly all incident blue light ($Abt\%_{465\ nm}$ = 97.0±0.8) and reflectance and transmission total only about 2%. Reflectance of seedling and submerged leaves is also very low (2% or less) but due to the noticeable transparency of the leaves to light, transmission is higher than in the surface leaves. $Abt\%_{465nm}$ was not significantly different in seedling leaves *vs*. submerged leaves (90.7±1.9% *vs.* 91.9±2.42% respectively). Absorptances of adult leaves are ≈15% higher and submerged leaves are ≈9% higher than the default Absorptance used by the WinControl software (AbtF = 0.84) and so the actual ETR is considerably higher than relative ETR (rETR).

3.4 Rapid Light Curves

Figure 1 shows plots of Photosynthesis (as POER) *vs*. Irradiance of submerged seedling, adult submerged and surface leaves of *Nymphaea caerulea* leaves collected at local midday (11:32 solar time). The Waiting-in-Line equation was fitted using non-linear least-squares fitting of Equation (1). PAM light curve data is based on 12 leaves for the seedling and 8 leaves for the submerged leaves and 8 for surface leaves and 9 different irradiance levels. Means ±95% confidence limits of E_{opt} and ETR_{max} and $POER_{max}$ of the fits are included in Table 2 along with the other statistics calculated from the rapid light curves. Relative ETR (rETR) was corrected to actual ETR using the RAT data in Table 1B and recalculated on a chlorophyll *a* (Chl *a*) basis using the Chl *a* m^{-2} data in Table 1A. ETR is expressed on a leaf surface area basis as mol e^- m^{-2} s^{-1} whereas photosynthesis on a Chl *a* basis is expressed as mol O_2 g^{-1} Chl *a* s^{-1}. The surface leaves saturated at high irradiances: the maximum photosynthesis on a surface area basis was high (E_{opt} = 923±68 µmol photon m^{-2} s^{-1}; ETR_{max} = 58.5±2.5 µmol e^- m^{-2} s^{-1}; $POER_{max}$ = 76.1±3.3 µmol O_2 g^{-1} Chl *a* s^{-1}) based on 9 different light intensities (thus 9 × 8 = 72 data points for surface and submerged leaves). Correlation coefficients were all r > 0.7467 giving p << 0.001 for all the P *vs.* E curve fits. The asymptotic photosynthetic efficiency (α_0) for surface leaves was 0.172±0.015 e^-/photon (Table 2). Submerged adult leaves are morphologically different to surface leaves and they have much lower chlorophyll *a* content on a surface area basis (Table 1B). Table 2 and Figure 2 show that they have substantially lower photosynthesis (ETR_{max} = 14.0±1.5 µmol e^- m^{-2} s^{-1}; $POER_{max}$ = 38.1±4.0 µmol O_2 g^{-1} Chl *a* s^{-1}) but the optimum irradiance is also much lower (E_{opt} = 419±64 µmol photon m^{-2} s^{-1}) resulting in a crucial change in *shape* of the POER *vs.* E curve. Photosynthetic efficiency was very low on a surface area basis (α_0 = 0.0978±0.0178 e^- $photon^{-1}$) compared to surface leaves

but on a Chl *a* basis was significantly higher than for surface leaves (α_0 = 0.261±0.046 O_2 photon^{-1} g Chl *a* m^{-2}). Seedling leaves are very small and thin even compared to subsurface leaves of adult plants (Table 1A). Table 2 and Figure 2 show that they have the lowest photosynthetic rate (ETR_{max} = 1.765±0.162 µmol e$^-$ m^{-2} s^{-1}; $POER_{max}$ = 4.946±0.455 µmol O_2 g^{-1} Chl *a* s^{-1}) and also a very low optimum irradiance (E_{opt} = 104±14 µmol photon m^{-2} s^{-1}) resulting in no substantial photosynthesis above about ¼ of sunlight. α_0 was much lower than mature submerged leaves growing adjacently (α_0 = 0.0460±0.0076 e$^-$ photon^{-1}; 0.129±0.021 O_2 photon^{-1} g Chl *a* m^{-2}) and extremely low compared to surface leaves. The α_0 of floating leaves is about 80% higher than submerged leaves on a surface area basis. On a Chl *a* basis, however, α_0 is highest in submerged leaves compared to adult surface leaves (Table 2). This is because surface leaves have a much higher Chl *a* content (Table 1A).

NPQ was calculated by the WinControl software based on the equations of Genty et al. [44], van Kooten and Snel [45] and Brestic and Zivcak [47] (Table 2). NPQ_{max} was calculated using non-linear least squares methods fitting to a simple exponential saturation model [53]. The number of valid data points may be substantially fewer than the measurements made in routine rapid light curves, for example in submerged leaves 72 yield determinations were made but only 64 produced estimates of NPQ (Table 2) (the Walz software gives an ERROR value if NPQ cannot be evaluated because of a division-by-zero error). NPQ results were highly variable and so it was difficult to determine NPQ_{max} or its exponential kinetic parameter (k_{NPQ} and hence ½ saturation point) by curve fitting. NPQ_{max} values were not very accurately measureable (seedling leaves ≈ 1.415, submerged leaves ≈1.2, surface leaves ≈ 1.81) with ½ saturation irradiances of ≈ 41, 69 and 214 µmol photons m^{-2} s^{-1} respectively. The kinetics NPQ could not be determined very accurately because of the limitations of the fits to a simple exponential saturation model: the maxima could be determined with reasonable accuracy (Table 2) but most NPQ values were measured at irradiances well

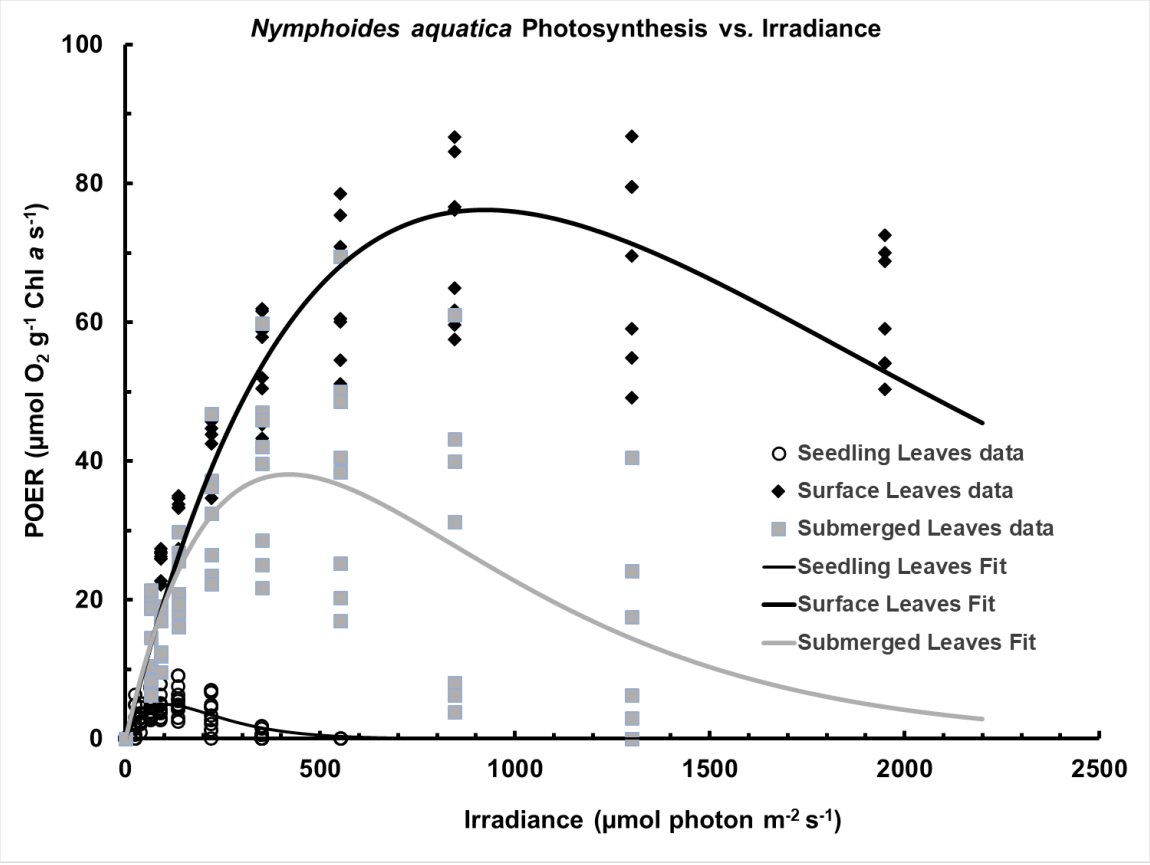

Figure 1. Plot of Photosynthetic Oxygen Evolution Rate (POER) *vs*. Irradiance of submerged seedling, adult submerged and surface leaves of *Nymphoides aquatica* leaves collected at local solar midday corrected from Thailand Standard Time. PAM light curve data are based on 12 surface, 8 submerged and 12 seedling leaves and 9 different irradiance levels. Means ±95% confidence limits of E_{opt} and $POER_{max}$ of the fits are included in Table 2 along with the other statistics calculated from the rapid light curves.

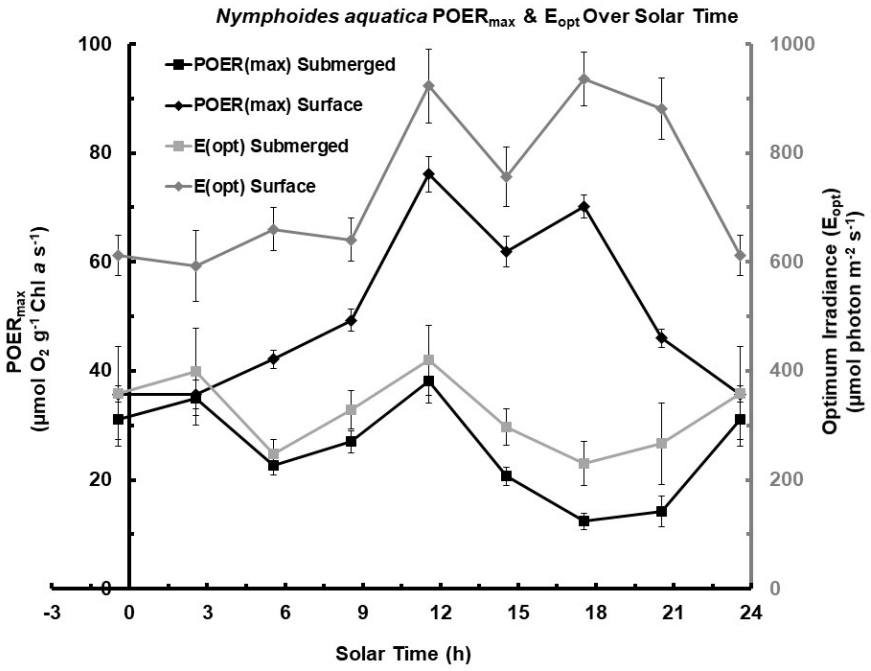

Figure 2. Photosynthetic Oxygen Evolution Rate ($POER_{max}$) and Optimum irradiance (E_{opt}) of surface and submerged *Nymphoides aquatica* leaves collected over the course of a day. Light period 6:00 to 18:15 solar time. The 24 h measurements are repeated twice on the graph (left and right) in order to show a complete diurnal cycle. Estimates of $POER_{max}$ (primary Y-axis) and E_{opt} (secondary Y-axis) are based on rapid light curves conducted at 3h intervals over the course of 24 h. Both types of leaves have a $POER_{max}$ and E_{opt} at about midday. There is a strong diurnal effect on $POER_{max}$ and E_{opt} on surface leaves with maxima at about midday and minimal values at night. The diurnal effect is less apparent in submerged leaves. There is a strong correlation between $POER_{max}$ and E_{opt} in both submerged and floating leaves. Means ±95% confidence limits (n = 8,72: eight leaves, 9 light levels in the rapid light curves).

above the half-saturation point and so the curvature to the exponential saturation curves could not be determined very accurately.

3.5 Temporal Changes in Photosynthesis

PAM measurements of photosynthetic parameters in surface and submerged *N. aquatica* show pronounced diel behaviour (Figures 2, 3 and 4) with generally higher E_{opt}, ETR_{max}, $POER_{max}$ and α_0 during the day and low values in the night. Diel differences in E_{opt} and $POER_{max}$ are much more pronounced in surface leaves compared to submerged leaves (Figure 2).

Figure 2 shows the $POER_{max}$ and E_{opt} irradiance of surface and submerged *N. aquatica* leaves collected over the course of a day at 3 h intervals. The same 24 h measurements are presented on the left and right on the graph in order to show a complete diurnal cycle. Estimates of $POER_{max}$ (primary Y-axis) and E_{opt} (secondary Y-axis) are based on rapid light curves conducted at 3 h intervals over the course of 24 h. The diurnal time-course $POER_{max}$ and E_{opt} curves are different in shape (Figure 2). There is a strong diurnal effect on $POER_{max}$ on surface leaves with a minima during midday and minimal values at night. The diurnal effect is less apparent in mature submerged leaves but there is still a midday minimum due to photoinhibition. The XYY format of the graph clearly shows that there is a strong correlation between $POER_{max}$ and E_{opt} in both submerged and floating leaves. There was not enough material available to investigate diurnal pattern in juvenile leaves.

Photosynthetic Efficiency (α_0) *vs.* Solar Time, where photosynthetic efficiency is expressed on a Chl *a* basis, is shown in Figure 3 based on data from Figure 2. For surface leaves, α_0 is at a maximum in the middle of the day and is lower at night (similar to findings in *Nymphaea caerulea* [18]). Photosynthetic efficiencies of submerged leaves are higher than the surface leaves during the night and during the day but significantly decrease over the course of the afternoon and so have a different diel response compared to surface leaves. Although there are some significant differences, α_0 on a Chl *a* basis is remarkably uniform: overall average photosynthetic efficiency is ≈0.2 (O_2 photon^{-1} m^2 g^{-1} Chl *a*) for floating leaves and submerged leaves. Figure 2 shows that $POER_{max}$ and E_{opt}

Table 2. Comparison of Photosynthesis of *Nymphoides aquatica* leaves using PAM for Plants at 11:33 solar time.

Parameter Class	Parameter	Seedling Leaves (n=12)	Submerged Leaves (n=8)	Surface Leaves (n=8)
Quantum Yield Photosystem II	Yield *vs*. Irradiance Pearsons r (n)	0.9797 (n=108)	0.9562 (n=72)	0.9708 (n=72)
	Yield (Y_{max})	0.657 ±0.025	0.670 ±0.048	0.549 ±0.024
	Yield (k) (µmol photon m^{-2} s^{-1})$^{-1}$	0.0717 ±0.008	0.0166 ±0.0023	0.0021 ±0.0002
Photosynthesis	ETR *vs*. Irradiance Pearsons (r)	0.7792	0.7467	0.9305
	E_{opt} (µmol photon m^{-2} s^{-1})	104 ±14	419 ±64	923 ±68
	ETR_{max} Surface Area Basis (µmol e^- m^{-2} s^{-1})	1.76 ±0.16	14.0 ±1.5	58.5 ±2.5
	$POER_{max}$ Chl *a* Basis (µmol O_2 g^{-1} Chl *a* s^{-1})	4.95 ±0.46	38.1 ±4.0	76.1 ±3.3
	PS Efficiency (α_0) Surface Area Basis (e^- $photon^{-1}$)	0.0460 ±0.0076	0.0958 ±0.0178	0.172 ±0.015
	PS Efficiency (α_0) Chl *a* Basis (O_2 $photon^{-1}$ m^2 g^{-1} Chl *a*)	0.129 ±0.021	0.261 ±0.046	0.226 ±0.019
Non-Photochemical Quenching	NPQ Pearsons r (n)	0.7979 (n=82)	0.5332 (n=64)	0.7446 (n=45)
	qNPQ ½ saturation (µmol photon m^{-2} s^{-1})	41.0 ±9.2	68.8 ±24.3	214 ±60
	NPQ_{max}	1.42 ±0.11	1.20 ±0.12	1.81 ±0.29

are strongly correlated. A plot of all $POER_{max}$ values *vs*. E_{opt} had a correlation of 0.9240 and $POER_{max}$ appears to be directly proportional to E_{opt} giving an overall α_{Eopt} value of 0.07120± 0.0021 O_2 $photon^{-1}$ m^2 g^{-1} Chl *a* or an α_0 value of 0.1935±0.0056 O_2 $photon^{-1}$ m^2 g^{-1} Chl *a*.

Figure 4 shows that the maximum of the parameter used to express Non-Photochemical Quenching (NPQ_{max}) varies over the diurnal cycle for both surface and submerged leaves. Daily maximum NPQ_{max} values were ≈ 1.415 for submerged seedling leaves, ≈1.21 for submerged leaves and ≈ 1.81 for surface leaves. Minimum NPQ_{max} values at night were ≈0.8. The diel patterns of NPQ_{max} over the course of 24 h of submerged leaves were different to those of surface leaves. There are limitations to the usefulness of NPQ measurements because of their limited reproducibility in *N. aquatica* and so should not be over-interpreted. There was a methodological difficulty with measurements in the present study for leaves collected during daylight. Photosynthetic electron transport of cut *N. aquatica* leaves was severely reduced in leaves given a routine dark preincubation treatment (see above and Appendix Table).

3.6 Titratable Acid and SAM/CAM Properties

Figure 5 shows the titratable acid of *N. aquatica* surface and submerged leaves collected over the course of a day. In surface leaves, titratable acid does not accumulate at night and decrease during the day as would be expected in a SAM/CAM plant. The lowest titratable acid was found at 08:33 (24.0±4.4 mol H^+ m^{-3}, n = 8) and the maximum value at 02:33 (31.0±9.1 mol H^+ m^{-3}, n = 8). These are not significantly different (p> 0.05). This result is similar to that found previously in *Nymphaea caerulea* [18] and contrary to what would be found if CAM physiology operated in the surface leaves of *N. aquatica.* In the case of submerged leaves, there is a more apparent diurnal

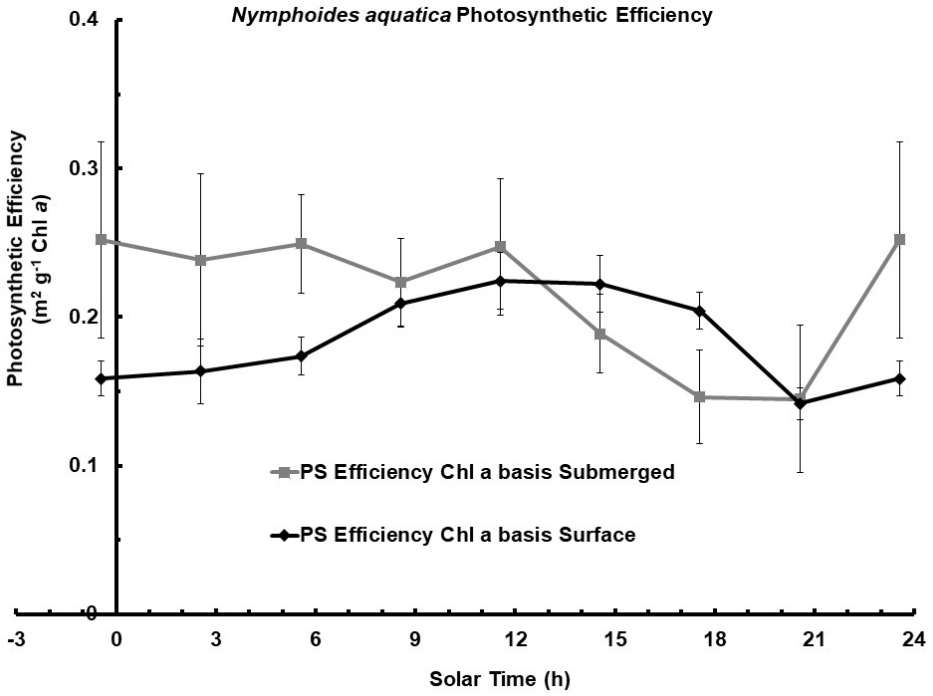

Figure 3. Photosynthetic Efficiency (α_0) of *Nymphoides aquatica* submerged and surface leaves collected over the course of a day based on the POER and E_{opt} data shown in Figure 2 and Table 2. Light period 6:00 to 18:15 solar time. For surface leaves the photosynthetic efficiency is at a maximum in the middle of the day and is lower at night. Photosynthetic efficiencies of submerged plants are higher than the surface leaves during the night and morning but significantly decreases in the afternoon. Means ±95% confidence limits.

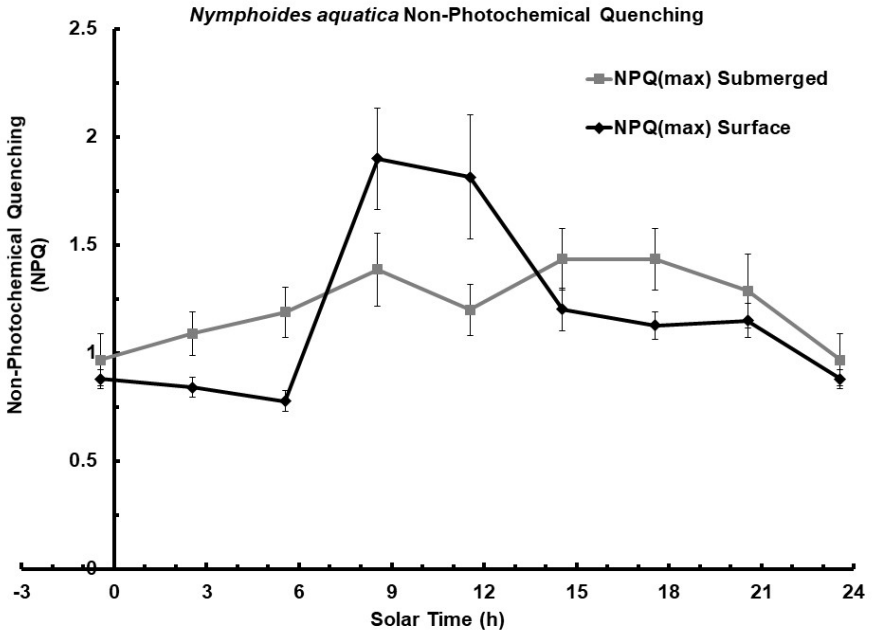

Figure 4. Non-Photochemical Quenching (NPQ) calculations on *Nymphoides aquatica* submerged and surface leaves collected over the course of a day, light period 6:00 to 18:15 solar time using the same data set as used for Figures 2 and 3. The asymptotic maximum (NPQ_{max}) were estimated using non-linear least-squares fitting of simple exponential saturation curves to NPQ *vs.* Irradiance. The largest differences between NPQ_{max} values were found during the morning in the surface and submerged leaves. Means ±95% confidence limits.

cycle of leaf acidity that it could be argued might be consistent with SAM/CAM physiology. The lowest titratable acid was found at 17:33 (19.0±4.9 µmol g^{-1} FW: 16.9±3.7 mol H^+ m^{-3}, n = 8) and the maximum value was at 11:33 (38.2±6.8 µmol g^{-1} FW: 34.0±5.1 mol H^+ m^{-3}, n = 8). These acidity values are significantly different ($p< 0.05$) but imply a maximum diurnal change on leaf acidity of only 19.0±7.6 µmol g^{-1} FW or 17.0±6.3 mol H^+ m^{-3} based on the water content of the leaves.

3.7 Estimating Primary Productivity

Primary productivity (P_g) is normally expressed as gC per m^2 per hour or per day and so the ETR data on a leaf surface area was converted into gC m^{-2} h^{-1} based on $4e^- \equiv 1O_2 \equiv 1C$. P_g of *N. aquatica* leaves (gC m^{-2} h^{-1}) over the course of a day was estimated using Equation (1) by first taking the calculated irradiance (*E*) for the summer solstice (22 June) at Phuket and then using the estimates of ETR_{max} and E_{opt} made during the course of the day (Figure 2). For example, taking the midday $POER_{max}$ of 14.63 µmol O_2 m^{-2} s^{-1} (76.1 µmol O_2 g^{-1} Chl *a* s^{-1}) for floating leaves (Table 2) this is equivalent to a maximum carbon fixation rate of 0.631 gC m^{-2} h^{-1} on a leaf surface area basis. As noted in the introduction POER gives a high estimate of gross photosynthesis (Pg) because it cannot take into account photorespiration. The results, calculated as described by Ritchie [18], shown in Figures 6a and b, were integrated using the trapezium rule to estimate cumulative and total daily P_g. Total daily irradiance on a clear day would be ≈57.4 mol photon m^{-2} d^{-1} (daily maximum PPFD 2100 µmol photon m^{-2} s^{-1}): total P_g increased rapidly during the morning but levelled off and strongly declined during the middle of the day because of photoinhibition during the middle of the day, followed by resumption of high photosynthesis in the afternoon. In the case of the submerged leaves, because of their much lower ETR_{max} than surface leaves and their low E_{opt} values, photosynthesis over the course of a day was much lower than the surface leaves and was very low in the middle of the day from 9:00 to 15:00 solar time (Figure 6a). The PAM data gives an estimation of the maximum rate of photosynthesis of ≈0.53 g C m^{-2} h^{-1} at about 08:00 solar time in the morning, a significant decrease to only ≈0.14 g C m^{-2} h^{-1} during the middle of the day, followed by a rise to ≈0.51 g C m^{-2} h^{-1} in the late afternoon (16:30). The PAM data gives an estimation of total daily photosynthesis of ≈3.7±0.6 g C m^{-2} d^{-1} or 19.5±2.9 g C g^{-1} Chl *a* d^{-1} for surface leaves but only ≈0.338±0.051 g C m^{-2} d^{-1} (≈3.68±0.61 g C g^{-1} Chl *a* d^{-1}) for submerged leaves because of their much lower E_{opt} and $POER_{max}$ (Figure 2).

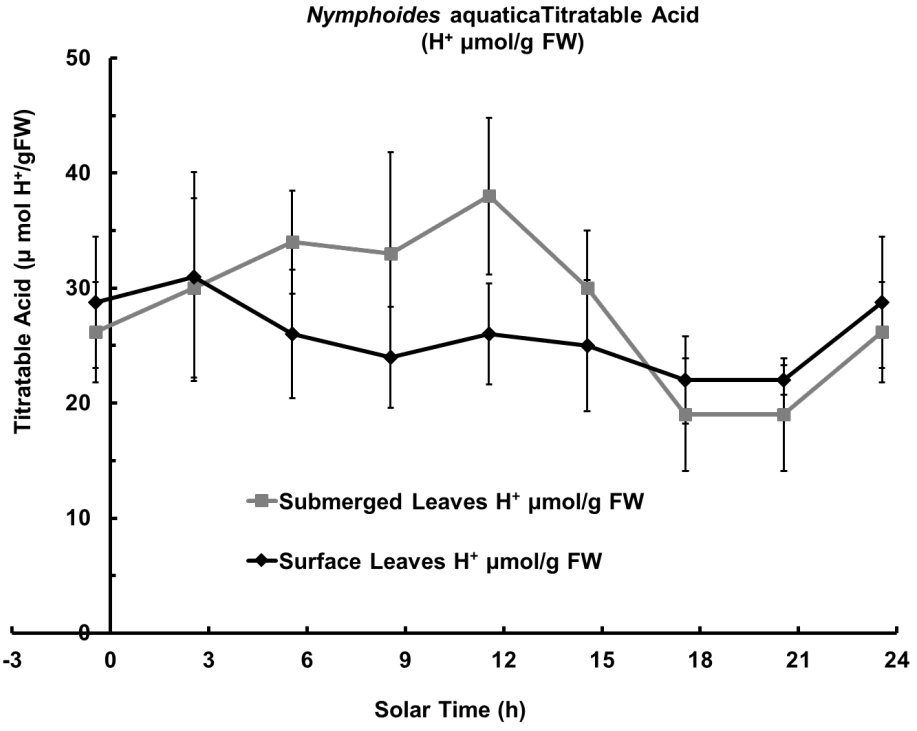

Figure 5. Titratable acid of *Nymphoides aquatica* surface and submerged leaves collected over the course of a day, light period 6:00 to 18:15 solar time. Data are means based on 8 replicates. Error bars are ±95% confidence limits. In surface leaves titratable acid does not accumulate at night and decrease during the day as would be expected in a SAM/CAM plant. In the case of submerged leaves there is a more apparent diurnal cycle of leaf acidity.

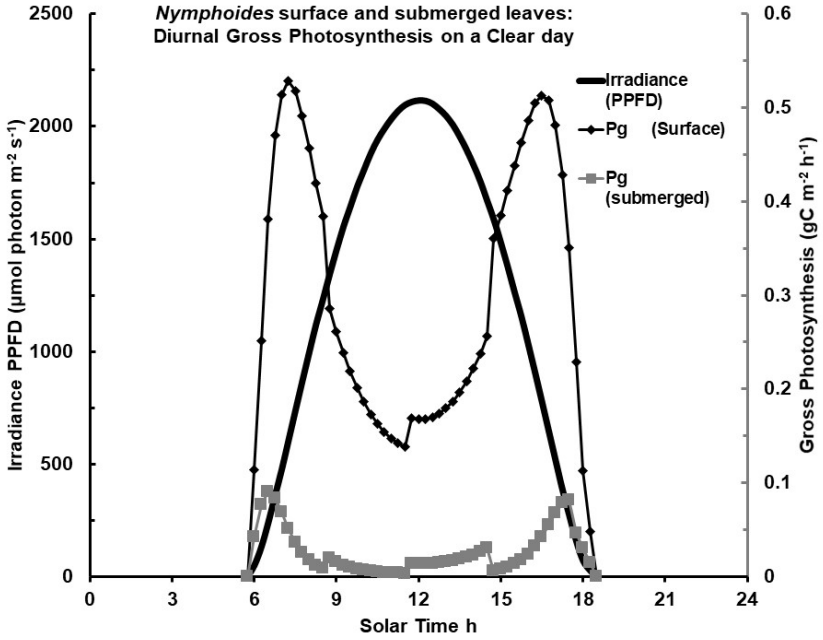

Figure 6a. Estimated total Gross Photosynthesis (P_g: gC m^{-2} day^{-1}) of *Nymphoides aquatica* leaves based upon ETR_{max}, $POER_{max}$ and E_{opt} data (Figure 2) inserted into Equation 1 and using the daily irradiance curve for a sunny day. Integration of the PAM data over time gives a total daily photosynthesis of about 3.71±0.56 gC m^{-2} day^{-1} from a total daily irradiance of 57.4 mol photon m^{-2} day^{-1} (PPFD) for a clear day. Low $POER_{max}$ and low optimum irradiance (Figure 2) results in high photoinhibition at high irradiances Gross photosynthesis by the submerged leaves and would be very low particularly during the middle of the day (9:00 to 15:00)

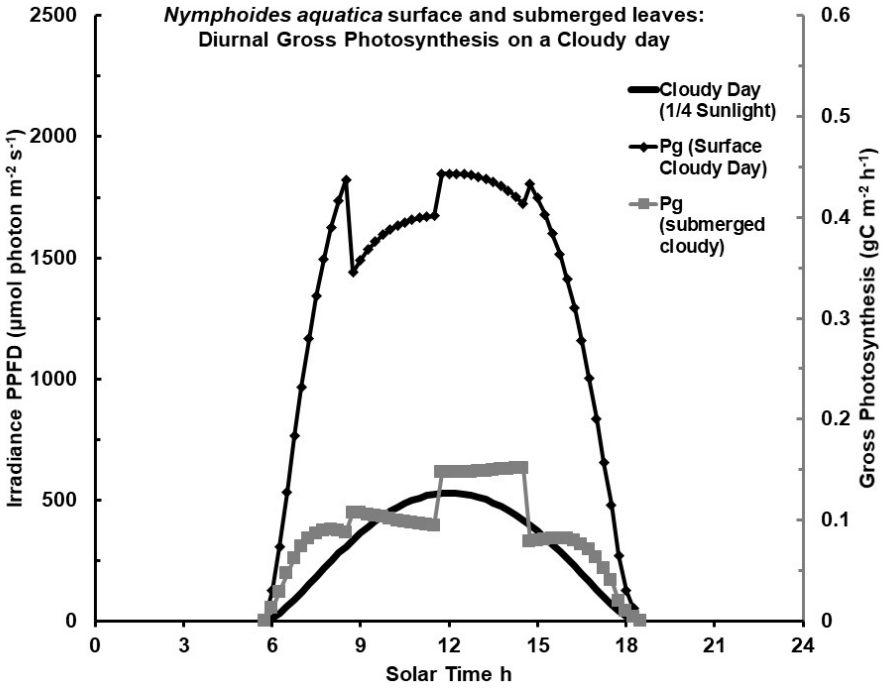

Figure 6b. Estimated total Gross Photosynthesis (P_g) of *Nymphoides aquatica* leaves calculated as for Figure 6a. P_g of submerged leaves greatly increased under cloudy conditions or under a canopy of floating leaves. Total daily irradiance would be about 14.3 mol photon m^{-2} for a cloudy day typical of the wet season. Reduced daily irradiance actually increased daily photosynthesis of surface leaves (≈ 4.1±0.6 gC m^{-2} d^{-1}) because midday photoinhibition was much reduced compared to Figure 6a and greatly increased the photosynthesis of submerged leaves.

On a cloudy day measurements of PPDF irradiance at midday was only about 500 μmol photon m^{-2} s^{-1} PPFD (Apogee Instruments Quantum Meter MQ-220, Apogee Instruments, Lothan, UTAH 84321, USA). Figure 6b shows that if daily irradiance was reduced by 75%, rather than decreasing photosynthesis the total daily photosynthesis would be greatly increased because midday photoinhibition is decreased. For a daily irradiance of 14.3 mol photon m^{-2} the total daily photosynthesis by the surface leaves was increased to 4.10±0.62 gC m^{-2} d^{-1} but photosynthesis of the submerged leaves increased to 1.16±0.17 gC m^{-2} d^{-1} or a quadrupling of their photosynthesis compared to a sunny day.

4. Discussion

Rapid light curves on *N. aquatica* ideally should be done on leaves *in situ* (as done for Oil Palm [42]). The 10 min dark pre-treatment routinely used in previous rapid light curve studies on pineapples, orchids, blue water lilies and *Davallia angustata* in previous studies in our laboratory was found to be unsuitable for *N. aquatica* see Appendix Table). The relationship of estimates of gross photosynthesis and net photosynthesis of anything but very small vascular plants such as *Lemna* and *Wolffia* is always problematic [48] but is especially the case for plants with aerenchyma. The respiration (and hence net photosynthesis) of the whole dwarf water lily plant would be very difficult to measure experimentally. In the present study leaves were cut from the plants and brought into the laboratory from outside the building and kept in the light in the laboratory for as short a time as practicable before being used for rapid light curves.

In chlorophyll content per unit surface area and absorptance properties the floating leaves of *N. aquatica* are comparable to that found for the floating leaf morphotype of *Potamogeton sp.* plants [5] and the floating leaves of the Blue Water Lily *Nymphaea caerulea* [18]. In their photosynthetic properties (Tables 1 and 2; Figures. 1, 2, 3, 4, 6a and 6b), the surface leaves of *N. aquatica* resemble those of *Nymphaea caerulea* [18,62] despite *N. aquatica* leaves having a marked wounding response encountered in the present study. The asymptotic photosynthetic efficiency (α_0) for surface leaves, on a surface area basis, was 0.172±0.015 e^-/photon (Table 2) is somewhat lower than a typical value found for C3 vascular plants [39,49,63] or CAM plants [40,41] but closely similar to that found previously in the Blue Water Lily [18]. Figure 2 (and analysis of $POER_{max}$ and E_{opt} data, see above) shows that there is a strong overall correlation between $POER_{max}$ and E_{opt}. A similar phenomenon was noted for the resurrection plant *Davallea angustata* [49]: $POER_{max}$ was appeared to be directly proportional to E_{opt} resulting in an essentially constant α_0 on a Chl *a* basis over a daily cycle. Such an observation should not be taken as a universal: in another study it has been found that the $POER_{max}$ and E_{opt} in the littoral weed species, *Launaea sarmentosa* exhibits no such close correlation [64].

Experimentally determined absorptances of *Nymphaea caerulea* leaves were not available when the study was published by Ritchie [18]. The Abt_{465nm} values (Abt_{465nm} = 98.2±0.2) found by Ritchie and Runcie [62] show that ETR and Pg of *Nymphaea caerulea* was underestimated by a factor of 98.2/84 or about 17% in the original study. Making allowances for this, the ETR_{max}, $POER_{max}$ and α_0 of surface leaves of *N. aquatica* have considerably lower ETR_{max}, $POER_{max}$ and photosynthetic efficiencies than *Nymphaea caerulea* [18] which would have a considerably higher photosynthetic rate than originally reported because its absorptance is above the default value of 0.84 [62].

The NPQ_{max} of mature submerged and surface leaves (Figure 4) are comparable to those found in other vascular plants (orchids [40,63], pineapples [41], blue water lily [18], *Wolffia arrhiza* [48], Oil Palm [42] and *Davallia angustata* [49]) but the high variability of NPQ means that NPQ data needs to be interpreted cautiously [47]. In the case of surface leaves NPQ_{max} tends to be maximum during the morning contrary to previously findings for *Dendrobium* orchids and pineapples [40,41] but in agreement with findings on *Nymphaea caerulea* [18]. Diel changes in Non-Photochemical Quenching (NPQ) have been noted in non-CAM plants [44,45,51] and in facultative CAM plants (*Clusia hilariana* [68], *Clusia minor* [24,25,26,69], *Mesembryanthemum crystallinum* [70] and obligate CAM species such as *Kalanchoë daigremontiana* and *K. pinnata* [66], *Dendrobium* orchids [40] and the Phuket pineapple [41]. In this study, lower NPQ_{max} values were found at dawn than in the rest of the day and during the night (Figure 4) (for *Nymphaea caerulea* see Ritchie [18]. High NPQ_{max} values were found in surface leaves in the morning until about midday then decreased (Figure 4); submerged leaves had a less conspicuous daylight/dark effect with minimal values at night and higher values during the day.

Diurnal cycling is a diagnostic feature of CAM physiology and is essential for CAM to function [21-26,40,41,68,69,71] but only certain diurnal cycling patterns are consistent with SAM/CAM physiology. The magnitude and diurnal patterns of leaf acidity found in the blue water lily [18] and the fern *Davallia angustata* [49] are not consistent with any significant CAM or SAM physiology. Obligate and facultative CAM plants and especially CAM-cycling type plants, use both the reservoir of CO_2 fixed as C4 acids during the previous night plus some atmospheric CO_2 taken

up while the stomates are still open in daylight as sources of CO_2 for the Calvin cycle. There is a wide spectrum of the expression of CAM physiology: some orchids express little or no significant CAM physiology (e.g. *Vanda sp.* [63]).

The diurnal pattern of titratable acid in the leaves of *N. aquatica* surface leaves is not consistent with any significant CAM physiology (Figure 5) consistent with previous findings on *Nymphaea caerulea* [18]. Keeley and Morton [4] also found no significant CAM physiology in the Yellow American Water Lily *Nuphar polysepalum*. The magnitude of changes in titratable acid is also too low for any significant CAM/SAM physiology. The amount of titratable acid in *N. aquatica* leaves (≈20 to 50 μmol H^+ g^{-1} FW, Figure 5) is lower than previously found in *Nymphaea caerulea* plants which were growing in the same lily pond bowls on the Phuket campus (≈ 60 to 82 μmol H^+ g^{-1} FW [18]). The acid content in the submerged *N. aquatica* leaves is also lower than found in *Nymphaea caerulea*. Classical CAM plants like *Dendrobium* orchids [40], pineapples [41] and *Clusia sp.* [24-26] and aquatic plants known to have SAM/CAM physiology (*Isoetes howellii* [7,13] and *Littorella uniflora* [9]) store ≈300 to over 1000 μmol H^+ g^{-1} FW on a diurnal cycle.

The surface leaves of *N. aquatica* do not show the diagnostic diurnal rhythm of nocturnal accumulation of acid in the leaves and metabolism of the stored C4 acids during the day (Figure 5) that is found in classic CAM plants [40,41]. As is the case in the leaves of *Nymphaea caerulea* [18], the surface leaves of *N. aquatica* do not perform CAM but the possibility remained that perhaps the submerged leaves performed some SAM/CAM physiology. Figure 5 does show that in submerged leaves there is some evidence for accumulation of acid at night and in the morning and a decrease in the afternoon but the labile organic acid pool of submerged leaves *N. aquatica* is too small to support significant CAM/SAM physiology. At midday the accumulated acid in submerged leaves was found to be 38.23±6.76 μmol H^+ g^{-1} FW (n = 8) or using the conversion factors in Table 1A, 34.0±5.1 mol m^{-3} or 4.945(±0.802) × 10^{-3} mol H^+ m^{-2}. At 17:33 at the end of daylight the titratable acid had fallen to 19.03±4.92 μmol H^+ g^{-1} FW or 16.90±3.69 mol H^+ m^{-3} on a leaf water basis or 2.462(±0.560) × 10^{-3} mol H^+ m^{-2}. The difference in acid content in the leaves over this 6h period is only 19.2±7.6 μmol H^+ g^{-1} FW; 17.0±6.3 mol H^+ m^{-3} or 2.48±0.93 μmol H^+ m^{-2}. Assuming the accumulated acid is malate (a diprotic C4 acid) then at midday the leaves had ≈17 mol malate m^{-3} which fell to ≈8.5 mol malate m^{-3} at sunset, which would be able to supply 1.24(±0.47) ×10^{-3} mol CO_2 m^{-2} for photosynthesis. From Figures 6a and b it can be estimated that the total carbon fixation by underwater leaves of *N. aquatica* from midday to sunset in full daylight can be no more than about 13.7(±2.1) × 10^{-3} mol C m^{-2} based on a C:O_2 ratio of 1 and integrating over time by the trapezium rule. This is much higher than the amount of CO_2 potentially stored in the vacuoles of the leaves and would supply only enough CO_2 for about 33±13 min of photosynthesis in full daylight. Photosynthesis on a cloudy afternoon by submerged leaves would total about 57.8(±8.7) × 10^{-3} mol C m^{-2} and so the leaves would exhaust the vascular CO_2 pool in only 7.7±3.1 min. Ritchie [18] calculated that vacuolar acid in *Nymphaea caerulea* could only supply enough CO_2 to account for only about 17 minutes of photosynthesis of the plant in full daylight.

Another approach to the problem shows that the amount of organic acid inside the submerged leaves of *N. aquatica* is not sufficient to support any significant CAM-like physiology. If we assume that floating leaves cover 90% of a pond surface, then the average light received by an understory of submerged leaves would be an irradiance of only about 10% of full sunlight [72] totalling about 5.74 mol photons m^{-2} d^{-1}. Daily carbon fixation would be about 1.4 gC m^{-2} d^{-1} or a total of 0.7±0.1 gC m^{-2} (59±8 mmol C m^{-2}) on a sunny afternoon. The leaves would exhaust the organic acids stored in the submerged leaves in only 8±3 minutes.

SAM/CAM physiology only occurs in submerged *Isoetes* and *Littorella* species [6,7,9,10,13]. Smits et al. [73] found that in terms of HCO_3^- usage the underwater leaves of Nymphaeid seedlings are quite different to adult floating leaves but we have shown that submerged *N. aquatica* leaves do not store enough C4 acids in their vacuoles to support SAM/CAM physiology. Photosynthesis of both submerged and surface leaves of *N. aquatica* shows definite diel cycles in most PAM parameters but the cycling pattern is not what would be expected in a CAM plant (Figures 2 to 4). Table 2 and Figures 2 and 3 show that surface leaves of *N. aquatica* are "sun leaves" with high rates of photosynthesis in full sunlight [43] but Nymphoid plants are not C4. Smits et al. [73] determined that the CO_2 compensation point of *Nymphaea alba*, *Nuphar lutea* and *Nymphoides peltata* leaf disks varied from 6.6 to 13.5 mmol CO_2 m^{-3}. These are typical C3 values, well above the essentially zero values found in C4 plants.

PAM fluorometers measure the light reactions of photosynthesis and provide only indirect information about the Calvin Cycle, ATP and NADPH+H^+ status or the source of the CO_2 used for carbon fixation. Slesak et al. [74] showed that in *Mesembryanthemum crystallinum* under conditions of high light, but little or no available CO_2, there is a build-up of NADPH+H^+ and H_2O_2 resulting in significant photosystem damage. The lack of suppression

of NPQ found in the present study of *N. aquatica* during the middle of the day agrees with previous observations on *Nymphaea caerulea* [18] and contrasts results on true CAM plants [40,41].

E_{opt} of *N. aquatica* of ≈850-1000 µmol photon m^{-2} s^{-1} PPFD (Table 2 and Figure 2, Appendix Table) classifies *N. aquatica* as a sun plant: *Nymphaea caerulea* saturates at similar irradiances ≈1000 µmol photon m^{-2} s^{-1} [18]. Figures 6a and b are plots of P_g *N. aquatica* using our ETR_{max} and E_{opt} data over the course of daylight (Figure 3). Irradiance reached over 2100 µmol m^{-2} s^{-1} at midday in Phuket resulting in substantial photoinhibition during the middle of the day. Compared to *Nymphaea caerulea*, midday inhibition is more severe in *N. aquatica* resulting in an estimated daily total gross photosynthesis of ≈3.71±0.51 gC m^{-2} d^{-1} on a full sun day but 4.1 ± 0.6 gC m^{-2} d^{-1} on a cloudy day compared to more than 6 gC m^{-2} d^{-1} in *Nymphaea caerulea* [18] when the original estimates are corrected to actual ETR rather than relative ETR (rETR) [62].

PAM fluorometers give no information on respiration: oxygen electrode, ^{14}C or IRGA methods are necessary to make estimates of respiration and hence net photosynthesis from PAM data [38,75,76]. Measurement of respiration of excised leaf disks and pieces of petiole of a water lily is *in principle* straightforward but misleading because the respiration of the whole plant, including the petioles, roots and rhizome is required including anaerobic respiration *in situ* [15,16,33,52]. Solid, liquid and gas phases, the internal ventilation system and aerobic and anaerobic compartments within the mud substrate all combine to make it very difficult to make estimates of respiration (and hence net photosynthesis) in a Nymphoid aquatic plant *in situ*. Inferences can be made about the magnitude of respiration *of the whole plant* if growth (Net Photosynthesis) is measured and good estimates are made of gross photosynthesis by a range of different methods.

The POER achievable by *N. aquatica* on a sunny day (≈3.71±0.56 gC m^{-2} d^{-1}; Figure 6a) is comparable to *Nymphaea caerulea* [18], wetland communities [77] and well-kept field C3 crops or pastures [43]. This is despite the relatively low photosynthetic efficiency of *N. aquatica* (Table 2; Figure 3) (compare to *Nymphaea caerulea* water lily [18], Oil Palm [42] and *Davallia angustata* [49]. POER for a *N. aquatica* pond in Phuket at the summer solstice in the wet season with overcast days with ≈500 µmol photon m^{-2} s^{-1} PPFD (or 1/4 full sunlight) would be about 10% higher (4.1±0.6 gC m^{-2} d^{-1}) due to less photoinhibition in the middle of the day [54]. Shading (75%) due to cloud cover which would reduce daily irradiance to ≈14.3 mol photon m^{-2} d^{-1} but the reduced irradiance would quadruple POER of submerged *N. aquatica* leaves to 1.16±0.17 gC m^{-2} d^{-1}. Shading of 90% actually increases the photosynthesis of submerged leaves even further (1.4±0.2 gC m^{-2} d^{-1}). The photosynthesis of a *N. aquatica* water lily bed with essentially 100% floating leaf cover would be considerably above the production by the floating leaves alone (3.7 gC m^{-2} d^{-1}) because of an additional contribution by the submerged leaves to add up to as much as ≈5 gC m^{-2} d^{-1}.

A water lily pond covered by Nymphoid floating leaf species has important structural differences to most photosynthetic plant communities [18,72] because it acts as a single flat leaf absorbing nearly all incident light (Table 1B) [72,78-81] but photoinhibition is a limitation for productivity for both floating and especially for submerged leaves. Even in a plant that rates as a sun plant based on its photosynthesis vs. irradiance curves (Figures 1 and 2), *N. aquatica* photosynthesis is greatly reduced at high irradiances during the middle of a sunny day and daily photosynthesis on a cloudy day turns out to be about the same as a sunny day because of reduced midday photoinhibition (Figures 6a and b).

Abbreviations

α_0, photosynthetic efficiency at asymptotically zero Irradiance; α_{Eopt}, photosynthetic efficiency at optimum Irradiance; E, Irradiance (µmol photon m^{-2} s^{-1}) 400-700 nm PPFD; ETR, electron transport rate; PAM, Pulse Amplitude Modulation fluorometry; PPFD Photosynthetic Photon Fluence Density (400 – 700 nm); POER, Photosynthetic Oxygen Evolution Rate; PSI, Photosystem I; PSII, Photosystem II; SAM, Submerged Aquatic Macrophyte.

Acknowledgements

The author wishes to thank Prince Songkla University – Phuket for providing facilities for the project. Tharawit WUTHIRAK gratefully acknowledges the support given for this project through the Science Achievement Scholarship Program of Thailand.

Conflicts of Interest

The authors declare no conflicts of interest.

References

[1] Les, D.H., Schneider, E.L., Padgett, D.J., et al., 1999. A Synthesis of Non-molecular, rbcL, matK, and 18S rDNA Data. Systematic Botany. 24, 28-46.

[2] Friis, E.M., Pedersen, K.R., Crane, P.R., 2001. Fossil evidence of water lilies (Nymphaeales) in the Early Cretaceous. Nature. 410, 357-360.

[3] Friis, E.M., Crane, P., 2007. New home for tiny aquatics. Nature. 446, 269-270.

[4] Keeley, J.E., Morton, B.A., 1982. Distribution of diurnal acid metabolism in submerged aquatic plants outside the genus *Isoetes*. Photosynthetica. 16, 546-553.

[5] Frost-Christensen, H., Sand-Jensen, K., 1995. Comparative kinetics of photosynthesis in floating and submerged *Potamogeton* leaves. Aquatic Botany. 51, 121-134.

[6] Keeley, J.E., Bowes, G., 1982. Gas exchange characteristics of the submerged aquatic Crassulacean Acid Metabolism Plant, *Isoetes howellii*. Plant Physiology. 70, 1455-1458.

[7] Keeley, J.E., 1983. Crassulacean Acid Metabolism in the Seasonally Submerged Aquatic *Isoetes howellii*. Oecologia. 58, 57-62.

[8] Keeley, J.E., Osmond, C.B., Raven, J.A., 1984. *Stylites*, a vascular plant without stomata absorbs CO_2 via its roots. Nature. 310, 694-695.

[9] Aulio, K., 1985. Differential expression of diel acid metabolism in two life forms of *Littorella uniflora*. New Phytologist. 100, 533-536.

[10] Webb, D.R., Rattaray, M.R., Brown, J.M.A., 1988. A preliminary survey for crassulacean acid metabolism in submerged aquatic macrophytes in New Zealand. New Zealand Journal of Marine & Freshwater Research. 22, 231-235.

[11] Maberley, S.C., Spence, D.H.N., 1989. Photosynthesis and photorespiration in freshwater organisms: amphibious plants. Aquatic Botany. 34, 267-286.

[12] Sharma, B.D., Harsh, R., 1995. Diurnal Acid Metabolism in the Submerged Aquatic Plant, *Isoetes tuberculata*. American Fern Journal. 85, 58-60.

[13] Keeley, J.E., 1998. CAM Photosynthesis in Submerged Aquatic Plants. Botanical Review. 64, 121-175.

[14] Snir, A., Gurevitz, M., Marcus, Y., 2006. Alterations in Rubisco activity and in stomatal behaviour induce a daily rhythm in photosynthesis of aerial leaves in the amphibious-plant *Nuphar lutea*. Photosynthesis Research. 90, 233-242.

[15] Laing, H.E., 1940. The Composition of the Internal Atmosphere of *Nuphar advenum* and other Water Plants. American Journal of Botany. 27, 861-868.

[16] Dacey, J.W.H., 1980. Internal Winds in Water Lilies: An Adaptation for Life in Anaerobic Sediments. Science. 210, 1017-1019.

[17] Allen, S.G., Idso, S.B., Kimball, B.A., 1990. Interactive effects of CO_2 and environment on net photosynthesis of water-lily. Agricultural Ecosystems & Environment. 30, 81-80.

[18] Ritchie, R.J., 2012. Photosynthesis in the Blue Water Lily (*Nymphaea caerulea* Saligny) using PAM fluorometry. International Journal of Plant Science. 173, 124-136.

[19] Troxler, T.G., Richards, J.H., 2009. $\Delta\delta^{13}C$, $\delta^{15}N$, carbon, nitrogen and phosphorus as indicators of plant ecophysiology and organic matter pathways in Everglades deep slough, Florida, USA. Aquatic Botany. 91, 157-165.

[20] Longstreth, D.J., 1989. Photosynthesis and photorespiration in freshwater emergent and floating plants. Aquatic Botany. 34, 287-299.

[21] Osmond, C.B., 1978. Crassulacean acid metabolism: curiosity in context. Annual Review of Plant Physiology. 29, 379-414.

[22] Ting, E.P., 1985. Crassulacean acid metabolism. Annual Review of Plant Physiology. 36, 595-622.

[23] Dodd, A.N., Borland, A.M., Haslam, R.P., et al., 2002. Crassulacean acid metabolism: plastic fantastic. Journal of Experimental Botany. 369, 569-580.

[24] Lüttge, U., 2004. Ecophysiology of Crassulacean Acid Metabolism (CAM). Annals of Botany. 93, 629-652.

[25] Lüttge, U., 2007. Photosynthesis. Lüttge, U. (ed) *Clusia: a woody Neotropical genus of remarkable plasticity and diversity*, 2nd edn. Ecological Studies. 194(8), 135-186. Springer, Berlin.

[26] Lüttge, U., 2008. *Clusia*: Holy grail and enigma. Journal of Experimental Botany. 59, 1503-1514.

[27] Pedersen, O., Sand-Jensen, K., 1992. Adaptations of submerged *Lobelia dortmanna* to aerial life form: morphology, carbon sources and oxygen dynamics. Oikos. 65, 89-96.

[28] Kaul, R.B., 1976. Anatomical observations on floating leaves. Aquatic Botany. 2, 215-234.

[29] Hough, R.A., Wetzel, R.G., 1977. Photosynthetic pathways of some aquatic plants. Aquatic Botany. 3, 297-313.

[30] Brewer, C.A., Smith, W.K., 1995. Leaf Surface Wetness and Gas Exchange in the Pond Lily *Nuphar polysepalum* (Nymphaeaceae). American Journal of Botany. 82, 1271-1277.

[31] Grosse, W., Mevi-Schutz, J., 1987. A beneficial gas transport system in *Nymphoides peltata*. American Journal of Botany. 74, 947-952.

[32] Grosse, W., Büchel, H.B., Tiebel, H., 1991. Pressurized ventilation in wetland plants. Aquatic Botany. 39, 89-98.

[33] Dacey, J.W.H., Klug, M.J., 1992. Ventilation by Floating Leaves in *Nuphar*. American Journal of Botany. 69, 999-1003.

[34] Grosse, W., Armstrong, J., Armstrong, W., 1996.

A history of pressurized gas-flow studies in plants. Aquatic Botany. 54, 87-100.

[35] Schreiber, U., Bilger, W., Neubauer, C., 1995. Chlorophyll fluorescence as a non-intrusive indicator for rapid assessment of *in vivo* photosynthesis. Schulze, E-D. and Caldwell, M.M. (eds) Ecophysiology of Photosynthesis: Ecological Studies. 100, 49-70. Springer, Berlin.

[36] White, A.J., Critchley, C., 1999. Rapid light curves: A new fluorescence method to assess the state of the photosynthetic apparatus. Photosynthesis Research. 59, 63-72.

[37] Rascher, U., Liebig, M., Lüttge, U., 2000. Evaluation of instant light-response curves of chlorophyll fluorescence parameters obtained with a portable chlorophyll fluorometer on site in the field. Plant, Cell & Environment. 23, 1398-1405.

[38] Franklin, L.A., Badger, M.R., 2001. A comparison of photosynthetic electron transport rates in macroalgae measured by pulse amplitude modulated chlorophyll fluorometry and mass spectroscopy. Journal of Phycology. 37, 756-767.

[39] Ritchie, R.J., 2008. Fitting light saturation curves measured using PAM fluorometry. Photosynthesis Research. 96, 201-215.

[40] Ritchie, R.J., Bunthawin, S., 2010. The Use of PAM (Pulse Amplitude Modulation) Fluorometry to Measure Photosynthesis in a CAM Orchid, *Dendrobium spp. (D.* cv. Viravuth Pink). International Journal of Plant Science. 171, 575-585.

[41] Ritchie, R.J., Bunthawin, S., 2010. The Use of PAM (Pulse Amplitude Modulation) Fluorometry to Measure Photosynthesis in Pineapple (*Ananas comosus* [L.] Merr). Tropical Plant Biology. 3, 193-203.

[42] Apichatmeta, K., Sudsiri, C.J., Ritchie, R.J., 2017. Photosynthesis of Oil Palm (*Elaeis guineensis*). Scientia Horticulturae. 214, 34-40.

[43] Atwell, B.J., Kreidermann, P.E., Turnbull, C.G.N., (eds), 1999. Plants in Action: adaptation in nature, performance in cultivation. Macmillan Education Publishers, South Yarra, Vic., Australia.

[44] Genty, B., Briantais, J.M., Baker, N.R., 1989. The relationship between the quantum yield of photosynthetic electron transport and quenching of chlorophyll fluorescence. Biochimica et Biophysica Acta. 990, 87-92.

[45] van Kooten, O., Snel, J.F.H., 1990. The use of chlorophyll fluorescence nomenclature in plant stress physiology. Photosynthesis Research. 25, 147-150.

[46] Holt, N.E., Fleming, G.R., Niyogi, N.K., 2004. Toward an understanding of the mechanism of non-photochemical quenching in green plants. Biochemistry. 43, 8281-8289.

[47] Brestic, M., Zivcak, M., 2013. PSII Fluorescence techniques for measurement of drought and high temperature stress signal in plants: protocols and applications. Rout, G,R, and Das, A,B, (eds) Molecular stress physiology in plants. 4, 87-131. (Springer, Dordrecht, The Netherlands).
DOI: https://doi.org/10.1007/978-81-322-0807-5

[48] Ritchie, R.J., Mekjinda, N., 2016. Arsenic Toxicity in the Water Weed *Wolffia arrhiza* Measured using Pulse Amplitude Modulation Fluorometry (PAM) Measurements of Photosynthesis. Ecotoxicology & Environmental Safety. 132, 178-187.
DOI: https://doi.org/10.1016/j.ecoenv.2016.06.004

[49] Quinnell, R., Howell, D., Ritchie, R.J., 2017. Photosynthesis of an Epiphytic Resurrection Fern *Davallia angustata* (Wall, ex Hook. & Grev.). Australian Journal of Botany. 65, 348-356.
DOI: http://dx.doi.org/10.1071/BT16222

[50] Krause, G.H., Weis, E., 1991. Chlorophyll fluorescence and photosynthesis: the basics. Annual Review of Plant Physiology. 42, 313-349.

[51] Schreiber, U., Endo, T., Mi, H.L., et al., 1995. Quenching analysis of chlorophyll fluorescence by the saturation pulse method: particular aspects relating to the study of eukaryotic algae and cyanobacteria. Plant & Cell Physiology. 36, 873-882.

[52] Smits, A.J.M., Laan, P., Their, R.H., et al., 1990. Root aerenchyma, oxygen leakage patterns and alcoholic fermentation ability of the roots of some nymphaeid and isoetid macrophytes in relation to the sediment type of their habitat. Aquatic Botany. 30, 3-17.

[53] Ritchie, R.J., 2015. Equation of Time Calculator. Available at www.researchgate.net/publication/282846329_Equation_of_Time. (verified 17 July 2016).
DOI: https://doi.org/10.13140/RG.2.1.4821.0642

[54] Ritchie, R.J., 2010. Modelling Photosynthetically Active Radiation and Maximum Potential Gross Photosynthesis. Photosynthetica. 48, 596-609.

[55] Gueymard, C.A., 1995. SMARTS, A simple model of the atmospheric radiative transfer of sunshine: algorithms and performance assessment. Professional Paper FSEC-PF-270-95, Florida Solar Energy Center, 1679 Clearlake Rd., Cocoa, FL, USA 32922.

[56] Gueymard, C.A., Myers, D., Emery, K., 2002. Proposed reference irradiance spectra for solar energy systems testing. Solar Energy. 73, 443-467.

[57] Ritchie, R.J., 2006. Consistent sets of spectrophotometric equations for acetone, methanol and ethanol solvents. Photosynthesis Research. 89, 27-41.

[58] Ritchie, R.J., 2015. Photosynthetic Light Curve Fitting Models. Available at www.researhgate.net/publication/283052624_Photosynthetic_Light_Curve_Fitting_Models (verified 26 May 2016).
DOI: https://doi.org/10.13140/RG.2.1.2301.7680

[59] McCree, K.J., 1972. The action spectrum, absorptance and quantum yield of photosynthesis in crop plants. Agricultural Meteorology. 9, 191-216.

[60] Björkman, O., Demmig, B., 1987. Photon yield of O_2 evolution and chlorophyll fluorescence characteristics at 77K among vascular plants of diverse origins. Planta. 170, 489-504.

[61] Frost-Christensen, H., Sand-Jensen, K., 1992. The Quantum Efficiency of Photosynthesis in Macroalgae and Submerged Angiosperms. Oecologia. 91, 377-384.

[62] Ritchie, R.J., Runcie, J.R.W., 2014. A portable Reflectance-Absorptance-Transmittance (RAT) meter for vascular plant leaves. Photosynthetica. 52, 614-626.
DOI: https://doi.org/10.1007/s11099-014-0069-y

[63] Sma-Air, S., Ritchie, R.J., 2020. Photosynthesis in a *Vanda sp* orchid with Photosynthetic Roots. Journal of Plant Physiology. 251, 153187.
DOI: https://doi.org/10.1016/j.jplph.2020.153187

[64] Ritchie, R.J., Sma-Air, S., Limsathapornkul, N., et al., 2021. Photosynthetic electron transport rate (ETR) in the littoral herb *Launaea sarmentosa* known as mole crab in Thailand. Photosynthesis Research. 150, 327–341.
DOI: https://doi.org/10.1007/s11120-021-00826-2

[65] Steele, J.H., 1962. Environmental control of photosynthesis in the sea. Limnology & Oceanography. 7, 137-150.

[66] Griffiths, H., Robe, W.E., Girnus, J., et al., 2008. Leaf succulence determines the interplay between carboxylase systems and light use during Crassulacean acid metabolism in *Kalanchoë* species. Journal of Experimental Botany. 59, 1851-1861.

[67] Zar, J.H., 2014. Biostatistical Analysis. 5th edition, Pearson New International Edition Pearson, Edinburgh Gate, Harlow, England, UK. pp. 761.

[68] Franco, A.C., Herzog, B., Hübner, C., et al., 1999. Diurnal changes in chlorophyll *a* fluorescence, CO_2-exchange and organic acid decarboxylation in the tropical CAM tree *Clusia hilariana.* Tree Physiology. 19, 635-644.

[69] Duarte, H.M., Lüttge, U., 2007. Circadian rythmicity. In: Lüttge, U. (ed) *Clusia: a woody neotropical genus of remarkable plasticity and diversity*, 2nd edn. Ecological Studies. 194(11), 245-256. Springer, Berlin.

[70] Broetto, F., Duarte, H.M., Lüttge, U., 2007. Responses of chlorophyll fluorescence parameters of the facultative halophyte and C3–CAM intermediate species *Mesembryanthemum crystallinum* to salinity and high irradiance stress. Journal of Plant Physiology. 164, 904-912.

[71] Cote, F.X., Andre, M., Folliot, M., et al., 1989. CO_2 and O_2 exchanges in the CAM plant *Ananas comosus* (L.) Merr. Determination of total and malate-decarboxylation-dependent CO_2-assimilation rates; study of light 0_2-uptake. Plant Physiology. 89, 61-68.

[72] Brock, T.C.M., Arts, G.H.P., Goosen, I.L.M., et al., 1983. Structure and annual biomass production of *Nymphoides peltata* (GMel.) O. Kuntze (Menyanthaceae). Aquatic Botany. 17, 167-188.

[73] Smits, A.J.M., de Lyon, M.J.H., van der Velde, G., et al., 1988. Distribution of three nymphaeid macrophytes (*Nymphaea alba* L., *Nuphar lutea* (L.) SM. and *Nymphoides peltata* (GMel.) O. Kunze in relation to alkalinity and uptake of inorganic carbon. Aquatic Botany. 32, 45-62.

[74] Slesak, I., Karpinska, B., Surówka, E., et al., 2003. Redox changes in the chloroplast and hydrogen peroxide are essential for regulation of C3–CAM transition and photooxidative stress responses in the facultative CAM plant *Mesembryanthemum crystallinum* L. Plant & Cell Physiology. 44, 573-581.

[75] Longstaff, B.J., Kildea, T., Runcie, J.W., et al., 2002. An *in situ* study of photosynthetic oxygen exchange and electron transport rate in the marine macroalga *Ulva lactuca* (Chlorophyta). Photosynthesis Research. 74, 281-293.

[76] Beer, S., Axelsson, L., 2004. Limitations in the use of PAM fluorometry for measuring photosynthetic rates of macroalgae at high irradiances. European Journal of Phycology. 39, 1-7.

[77] McCormick, P.V., Shuford, R.B.E., Backus, J.G., et al., 1998. Spatial and seasonal patterns of periphyton biomass and productivity in the northern Everglades, Florida, U.S.A. Hydrobiologia. 362, 185-208.

[78] Friend, A.D., 2001. Modelling canopy CO_2 fluxes: are "big leaf" simplifications justified? Global Ecology & Biogeography. 10, 603-619.

[79] Filbin, G.J., Hough, R.A., 1983. Specific leaf area, photosynthesis, and respiration in two sympatric Nymphaeaceae populations. Aquatic Botany. 17, 157-165.

[80] Madsen, T.V., Sand-Jensen, K., 1991. Photosynthetic carbon assimilation in aquatic macrophytes. Aquatic Botany. 41, 5-40.

[81] Falkowski, P.G., Raven, J.A., 2007. Aquatic photosynthesis, 2nd edn. Princeton University Press, Princeton, NJ, USA.

Appendix Table. Statistics on *Nymphoides aquatica* Pretreatment Times in Light and Dark

Experiment	Fm'	Y_{max}	Y_k	$Y_{0.5}$	r & P	E_{opt}	$POER_{max}$	Alpha α_0	r & P
zero dark	1236	0.6544	0.001696	408.7	0.9683	714.5	96.3	1.465	0.8945
n = 8	± 185	± 0.0236	± 0.000169	± 40.8	<< 0.001	± 68.7	± 4.9	± 0.159	<< 0.001
15 min dark	1494	0.6098	0.005072	136.6	0.8931	619.3	46.0	0.808	0.8220
n = 8	± 198	± 0.0487	± 0.000858	± 23.1	<< 0.001	± 70.8	± 3.0	± 0.107	<< 0.001
30 min dark	1362	0.5950	0.005420	127.9	0.9609	554.2	39.8	0.780	0.9720
n = 8	± 107	± 0.0371	± 0.000702	± 16.6	<< 0.001	± 24.5	± 1.1	± 0.041	<< 0.001
1h dark	1701	0.6185	0.007189	96.4	0.9217	474.8	35.0	0.801	0.9002
n = 8	± 221	± 0.0450	± 0.00111	± 14.9	<< 0.001	± 44.8	± 1.7	± 0.085	<< 0.001
2h dark	867	0.6058	0.007938	87.3	0.9307	432.8	30.4	0.763	0.9486
n = 16	± 352	± 0.0226	± 0.000696	± 7.7	<< 0.001	± 21.2	± 0.92	± 0.044	<< 0.001
Light Treatment									
Control									
0 h Light	947	0.6295	0.001300	533.1	0.98554	855.8	119	1.505	0.9811
n = 8	± 108	± 0.0121	± 0.000075	± 30.8	<< 0.001	± 47.2	± 3.1	± 0.092	<< 0.001
1h Light	1229	0.6533	0.001829	379.1	0.9757	732.5	93.5	1.388	0.9754
n = 8	± 143	± 0.0200	± 0.000151	± 31.4	<< 0.001	± 38.3	± 2.6	± 0.082	<< 0.001

Appendix Table Legend:

Experiments on cut leaves incubated in the dark showed that E_{opt} and ETR_{max} decreased over time if the leaves were kept in the dark. All values are means ± 95% confidence limits. Fm' is the fluorescence in the light acclimated state after a flash of actinic light and is used to calculate the Yield (Y = 1 – Fo/Fm') where, Fo is the fluorescence in the modulated measuring light (Genty et al. [44]; Brestic and Zivcak [47]). Y_{max} is maximum Yield (Y) fitted from a Y *vs.* Irradiance rapid light curve 0 to 1300 µmol photon m^{-2} s^{-1}. Y_k is the exponential constant fitted to the simple exponential decay curve fitted to the Y *vs.* Irradiance data; $Y_{0.5}$ is the irradiance at which Y was ½ maximum. r is the correlation coefficient, all r values were significant at p << 0.001. E_{opt} is the optimum irradiance of photosynthetic electron transport in µmol photon m^{-2} s^{-1} of the fitted waiting-in-line relationship of POER vs. Irradiance. $POER_{max}$ is the maximum photosynthetic electron transport rate (µmol O_2 g^{-1} Chl *a* s^{-1}) at the E_{opt} irradiance value in Alpha (α_0) is the photosynthetic efficiency at zero irradiance. The results show that photosynthesis in *N. aquatica* is very vulnerable to a wounding effect on excised leaves and so pre-incubation (light or dark) before rapid light curves is not appropriate in this species. Furthermore, since both $POER_{max}$ and E_{opt} both change over time the shape of the P *vs.* E curves of cut leaves changed over time. Preincubation in the dark is worse than cutting the leaves and keeping them in the light in the laboratory. Measuring rapid light curves as soon as possible after collection and keeping in the light was the best option for this species.

BILINGUAL
PUBLISHING CO.
Pioneer of Global Academics Since 1984

Tel.:+65 65881289
E-mail: contact@bilpublishing.com
Website:ojs.bilpublishing.com

2630-5054
03
9 772630 505224